

**WAVELET REPRESENTATION OF SENSOR  
SIGNALS FOR MONITORING  
AND CONTROL**

By

**VINOD KUMAR RAGHAVAN**

Bachelor of Technology

Osmania University

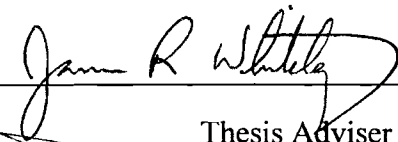
Hyderabad, Andhra Pradesh, India

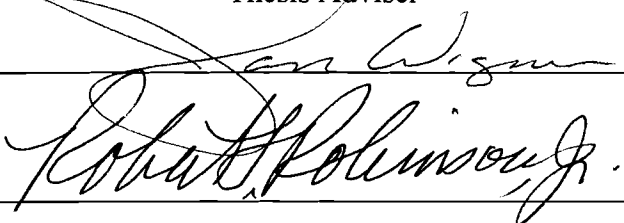
1992

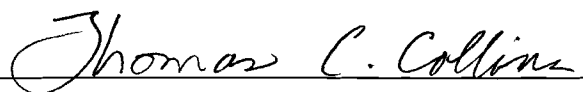
Submitted to the Faculty of the  
Graduate College of the  
Oklahoma State University  
in partial fulfillment of  
the requirements for  
the Degree of  
**MASTER OF SCIENCE**  
May, 1995

**WAVELET REPRESENTATION OF SENSOR  
SIGNALS FOR MONITORING  
AND CONTROL**

Thesis Approved:

  
\_\_\_\_\_  
Thesis Adviser

  
\_\_\_\_\_  
Robert H. Robinson, Jr.

  
\_\_\_\_\_  
Dean of the Graduate College

## PREFACE

The chemical Process Industries rely heavily on pattern based information utilization. Process trends and patterns contain virtually all the information about the process and provide the operators a basis to determine the process condition. It is based on changes in these patterns that operators make the necessary adjustments to the process operating conditions, depending on their interpretation. In general, process condition can confidently be judged only by monitoring multiple signals simultaneously and by context dependent pattern recognition. A simple example of a exothermic CSTR can be used to illustrate this. When the reactor temperature rises and the coolant flow rate remains constant or decreases, the operator may take it as a premonition of impending doom, but if the coolant flow rate also goes up to accommodate for this increase in reactor temperature, the operator might take no prophylactic measures. It can easily be concluded that good signal processing techniques are necessary to develop the next generation of automated process monitoring techniques.

Sensor signals samples are periodically collected by data collecting techniques that usually introduce sensor noise to the already noisy raw signal from the process. This raw signal has to be converted to a useful form before it can actually be used further. The challenge is to provide a signal processing technique that can process a signal on-line and feed it to a process monitoring technique. However, the catch is that all signal processing cause signal distortion at least to some extent. This cannot be tolerated, especially distortions towards the end of the signal, samples that correspond to the most recent juncture in time. This is because it is these samples that trigger off a process monitoring technique into predicting the process as normal or abnormal. Prediction of a normal state

as abnormal can probably tolerated but predicting an abnormal state as normal can prove catastrophic.

In this work a novel signal processing method using Wavelets is discussed. Wavelet Transforms are similar to the age old Fourier Transforms, but outmatches the Fourier Transforms in many desired attributes. Wavelets not only provide a powerful signal processing/analysis technique, they are also capable of providing significant data compression. In this work data compression's of the order of 90% were achieved without significant loss in the information content of the signals.

This work to our knowledge is the first to emphasize the importance of signal extension techniques for an applications like pattern recognition. A new signal extension technique (NET) is described and its superiority over other signal extension techniques is demonstrated.

I wish to thank Dr. James R. Whiteley for providing me the opportunity to work on this project. As my adviser on this project and a guide in many other issues, he provided me with guidance and support constantly. I am also grateful to him for lending an ear whenever I needed advise and support on personal issues too. I also wish to thank Dr. Arland H. Johannes and Dr. Jan Wagner for serving on my thesis committee.

I would also like to take this opportunity to thank Jack DeVeaux, Bruce Colgate at PDC Center of the Phillips Petroleum Co., Bartlesville and Tommy Long, Ben Mackay and Barbara Barton at the Phillips Refinery in Borger, TX, for their co-operation. I am also indebted to the School of Chemical Engineering, Oklahoma State University for providing me financial support.

Thanks are also due to my friends for their constant moral support. I wish to express my gratitude to my family, especially to the person who made everything possible, my mother. Special thanks are also due to Mrs. Ann Whiteley, for her painstaking review of this thesis.

I dedicate this thesis to the fond memory of my uncle, Mr. K.G. Murali Babu.

## TABLE OF CONTENTS

Chapter	Page
I. INTRODUCTION .....	1
Thesis Outline .....	2
II. SIGNAL ANALYSIS .....	3
Introduction .....	3
Signal Representation .....	4
The Fourier Transform .....	6
Discrete Wavelet Transforms .....	7
Analogy to Fourier Transforms .....	7
III. WAVELET TRANSFORMS .....	12
Introduction .....	12
Dilation Equations .....	12
Wavelet Construction .....	17
Computing the Scaling Function and Wavelet Coefficients .....	17
The Daubechies Family .....	21
Construction of the Scaling Function and Wavelet .....	26
Computing the decomposition coefficients .....	32
Multi-Resolution Analysis .....	35
Summary .....	38
IV. SIGNAL EXTENSION .....	47
Need for signal extension for sensor signals from	
Chemical Processes .....	39
Common signal extension methods .....	40
Circular Extension .....	40
Symmetric Extension .....	41

Chapter	Page
Padding with Zeros . . . . .	42
Padding with a constant value . . . . .	43
Summary of conventional extension methods . . . . .	44
The New Extension Technique . . . . .	45
NET1 . . . . .	46
NET2 . . . . .	48
NET3 . . . . .	48
NET4 . . . . .	49
Demonstration of NET technique . . . . .	54
Case I . . . . .	54
Case II . . . . .	58
Case III . . . . .	60
V. CONCLUSIONS . . . . .	65
Recommendations and Future work . . . . .	67

## LIST OF TABLES

Table	Page
I. Scaling function Coefficients for the Daubechies Family of Wavelets .....	29

## LIST OF FIGURES

Figure.	Page
1. A Sampled Process Signal . . . . .	5
2. Fourier Coefficients of the Process Signal in Figure 1 . . . . .	7
3. Fourth order Daubechies family scaling function and wavelet. . . . .	8
4. Wavelet Transform on a time-frequency scale . . . . .	9
5. Comparison of Fourier Decomposition and Wavelet Decomposition . . . . .	10
6. Illustration of a Wavelet at different dilations and translations . . . . .	14
7. The dyadic sampling of a Wavelet grid . . . . .	14
8. Figure showing some Wavelet Families . . . . .	16
9. The Box Function . . . . .	18
10. The Haar Wavelet and its dilates and translates . . . . .	19
11. The Hat Function . . . . .	20
12. Wavelet associated with the Hat function . . . . .	20
13. Scaling Functions associated with Daubechies Wavelets . . . . .	30
14. Daubechies Wavelets . . . . .	31
15. A basic decomposition and reconstruction representation . . . . .	32
16. Depiction of a MRA algorithm . . . . .	35
17. Representation of a Signal Decomposition upto three levels . . . . .	37



18.	Periodic Extension Technique . . . . .	40
19.	Example of periodic extension . . . . .	41
20.	Symmetric Extension Technique . . . . .	41
21.	Example of symmetric extension . . . . .	42
22.	Extension with Zeros . . . . .	43
23.	Example of extension with zeros . . . . .	43
24.	Extension with the boundary value . . . . .	44
25.	Example of extension with a constant value . . . . .	44
26.	The New Extension Technique . . . . .	47
27.	Different Extension Methods . . . . .	50
28.	Representation of Effect of Signal Extension on Signal Combination. Case I. . . . .	56
29.	Case II. . . . .	59
30.	Case III . . . . .	62

## SUMMARY OF NOMENCLATURE

$\delta(t)$	A unit impulse response
$f(t)$	Real time representation of a signal
$\alpha_k, \beta_k$	Decomposition basis functions
$g_k, h_k$	Decomposition coefficients of $\alpha_k, \beta_k$ respectively
$\varphi(t)$	Scaling function
$\psi(t)$	Wavelet
$c_k$	Scaling function coefficients
$d_k$	Wavelet coefficients
$\hat{f}(\xi)$	Fourier transform of $f(t)$
$m_0(\xi)$	A periodic function
H	High pass filter
G	Low pass filter
$a_j^i$	$j^{th}$ blurred decomposition coefficient at the $i^{th}$ decomposition level
$b_j^i$	$j^{th}$ detail decomposition coefficient at the $i^{th}$ decomposition level
$f_i$	Mean of $i$ signal samples
$M_i$	Mean squared deviation of $i$ signal samples

# **CHAPTER I**

## **INTRODUCTION**

The process industries rely heavily on pattern-based information utilization. Robust feature extraction and pattern recognition techniques are essential for the successful automation of a chemical process plant. Pattern based monitoring techniques require compact representation of the sensor data. In this work we describe a wavelet technique that provides efficient signal representation and trend pattern extraction.

Sensor signals in general are heavily marred by noise. Noise can mask the actual signal trend and make pattern recognition and feature extraction difficult. To enable better trend resolution, signals are analyzed using different techniques, e.g. the Fourier transform. The disadvantage of using conventional signal processing techniques such as the Fourier transform is that they are ineffective at handling localized signal behavior. Loss of a vital piece of information can be unacceptable for monitoring and control purposes. Wavelet transforms provide localized signal processing capability and better trend pattern representation.

All signal extension methods require the signal to be extended to prevent trend distortions. This work identifies the drawbacks of common signal extension methods and recommends a more effective method of signal extension.

Critical factors such as the wavelet family used, the number of levels of signal decomposition, and possible data compression techniques have also been explored. A detailed description of these topics is beyond the scope of this work, however.

## **Thesis Outline**

The organization of this thesis is as follows, Chapter II describes signal analysis techniques in general with special emphasis on Fourier and wavelet transforms. This chapter also discusses time-frequency relationships and introduces the concept of multi-resolution analysis.

Chapter III discusses general mathematical details of wavelets and wavelet transforms. Special mention is made of the Daubechies family of wavelets. This wavelet family is used extensively in this work. This chapter also presents the concept of multi-resolution analysis from a theoretical perspective.

Chapter IV is the main body of this work. It presents an overview of common signal extension methods and describes their shortcomings when used with wavelet transforms for pattern recognition and feature extraction applications. New signal extension methods are presented which avoid the problems with traditional techniques. Performance of these new methods is illustrated with case studies.

Chapter V concludes with a summary of this work and sets forth recommendations for future study.

## **CHAPTER II**

### **SIGNAL ANALYSIS**

#### **Introduction**

Signals are commonly analyzed by decomposing them into their frequency components. Frequency components are portions of the signal with different energies. Portions with higher energies correspond to the higher frequencies and, likewise, lower frequencies correspond to lower energy. A sound method for signal analysis requires detection and explicit representation of the temporal features in a joint time-frequency space. The ultimate objective of signal processing is to provide a unique signal representation.

The high frequency part of a signal is generally measurement noise and can be eliminated to the desired degree by passing it through a low pass filter. Filtering, in signal processing parlance, is analogous to physical filtering, e.g. separation of suspended impurities from a liquid. A low pass filter is one that allows the low frequency components of the signal to pass through. Low frequencies form the basic trend patterns of the signal. High pass filters do the opposite.

Signal processing techniques should avoid distortion of process trend, otherwise the interpretation of the trend by a process monitoring technique may be erroneous. Desirable qualities of a signal processing technique for trend extraction include the following :

- The technique should have the ability to analyze a signal over numerous resolution levels and capture the essential features of the process trend.
- The processing technique should ensure that there is neither (a) over-sampling which results in information redundancy, or (b) under-sampling which could result in information loss.
- The technique should be able to treat local behavior as a local, not global event. For example, if a sudden impulse in the process trend shows up sharply on the sensor reading, this is generally indicative of a valve failure, etc. Analyzed using a global technique, e.g. the Fourier transforms, the processed signal could show a more sluggish change like a load change. This representation is misleading.
- The signal analysis technique should provide a unique signal representation immune to signal translations i.e., the signal translated in time should provide a representation identical to the original representation, but translated appropriately.

### Signal Representation

If  $f^n$  is a sampled data representation of a sensor trend pattern containing  $N$  samples, then  $f$  can be expressed as shown below:

$$f(t) = \sum_{n=0}^{N-1} p_n \delta(t - n) \quad , t=0 \dots N-1 \quad (1)$$

and where  $\delta(n)$  is defined as a unit impulse response and has a value

$$\delta(\chi) = \begin{cases} 1 & \text{if } \chi = 0 \\ 0 & \text{otherwise} \end{cases} \quad (2)$$

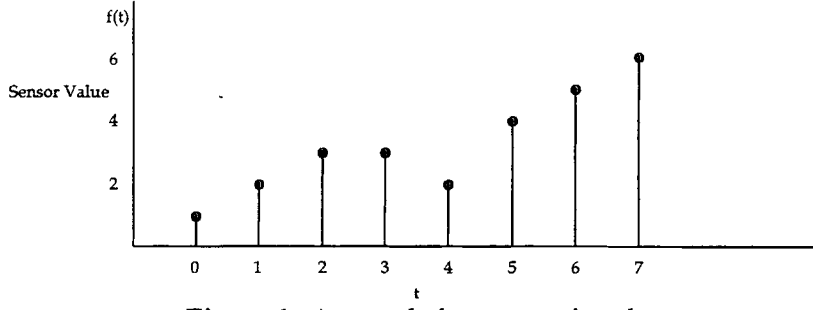


Figure 1: A sampled process signal.

In Figure 1, an 8 point signal is depicted. The trend pattern can be expressed using a time domain representation by a vector of coefficients  $p_n$ .

$$f(t) = \sum_{n=0}^7 p_n \delta(t - n), \quad (3)$$

where  $p=[1 \ 2 \ 3 \ 3 \ 2 \ 4 \ 5 \ 6]^T$ .

The signal in Figure 1 is localized in time using a time domain representation because it is expressed as a series of impulses in time. The magnitude (the sensor reading in this case) of an impulse gives the exact signal value at that instant of time. Frequency localization can be achieved by employing a Fourier transform to identify the frequency components that constitute the signal.

There are a number of other ways this signal can be represented. In general, the signal can be expressed by a pair of basis functions  $\alpha$  and  $\beta$ . The signal can be expressed as the sum of its decomposition products, or

$$f(t) = \sum_k g_k \alpha_k(t) + \sum_k h_k \beta_k(t) \quad (4)$$

where  $k$  is an index that defines the length of the signal.

The basis functions vary depending on the nature of the decomposition method adopted, and  $g_k$  and  $h_k$  are the decomposition coefficients associated with  $\alpha(t)$  and  $\beta(t)$ , respectively.

The most common signal analysis techniques are discrete Fourier transforms, discrete cosine transforms and, more recently, discrete wavelet transforms. The remainder of this chapter describes two methods: Fourier transforms and wavelet transforms. The Fourier transform [Bracewell, 1965; Brigham, 1974; Weaver, 1983] is described in detail to facilitate easier understanding of wavelet transforms.

### The Fourier transform

In the Fourier transform, the basis functions in equation (4) are sine and cosine functions. The Fourier transform decomposes the signal into sines and cosines of different frequencies and amplitudes, and these functions collectively form the original signal. For Fourier transforms,  $h$  and  $g$  in equation (4) are sine and cosine amplitude coefficients.

The mathematical representation of Fourier decomposition of a signal  $f(t)$  is

$$f(t) = \sum_k g_k \cos(tk) + \sum_k h_k \sin(tk) \quad (5)$$

An alternative representation of the Fourier transforms (FT) is

$$\text{FT}(f) = \int f(t) e^{-2j\pi ft} dt \quad (6)$$

Though powerful and popular, Fourier representations have some serious limitations [Bracewell, 1965; Brigham, 1974; Weaver, 1983]. They do not provide easy insight into the time domain behavior of the original signal which is essential for trend pattern representation. Figure 2 shows the time domain decomposition representation of the



process signal in Figure 1. This representation is generally inadequate for trend pattern representation and process monitoring for applications other than vibration monitoring. This limitation comes about from the fact that the analyzing functions in the Fourier transform are global in nature.

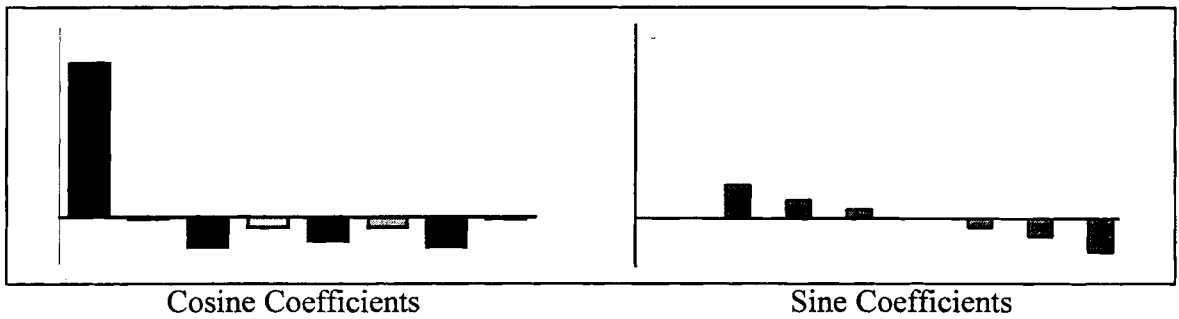


Figure 2: Fourier coefficients of the process signal in Figure 1

There are at least two ways to overcome this drawback. The first solution is to introduce time dependency in Fourier transforms so that the signal is analyzed, not on a global scale, but within windows in time [Akansu and Haddad, 1993; Chui, 1992b]. Another way of handling this problem is to use other basis functions that are more concentrated in time. This is where wavelet transforms come into the picture. They use analyzing functions that are localized in time.

### Discrete wavelet transforms

Wavelet transforms [Chui, 1992a; Chui, 1992b; Cohen *et al.*, 1992a; Daubechies, 1988; Daubechies, 1990; Daubechies, 1992; Mallat, 1989a; Mallat, 1989b; Strang, 1989] enable analysis in both time and frequency.

**Analogy to Fourier transforms:** In the same manner as sines and cosines in the Fourier transforms, wavelets and scaling functions form the basis functions in the wavelet

transforms. A key difference is that while sines and cosines have simple analytic expressions, scaling functions and wavelets are complex functions which are derived rather than naturally occurring. Wavelet decomposition of a signal is also represented by equation (4), where

$\alpha_k(t)$  is the scaling function

$\beta_k(t)$  is the wavelet

A sample scaling function and wavelet is shown in Figure 3.

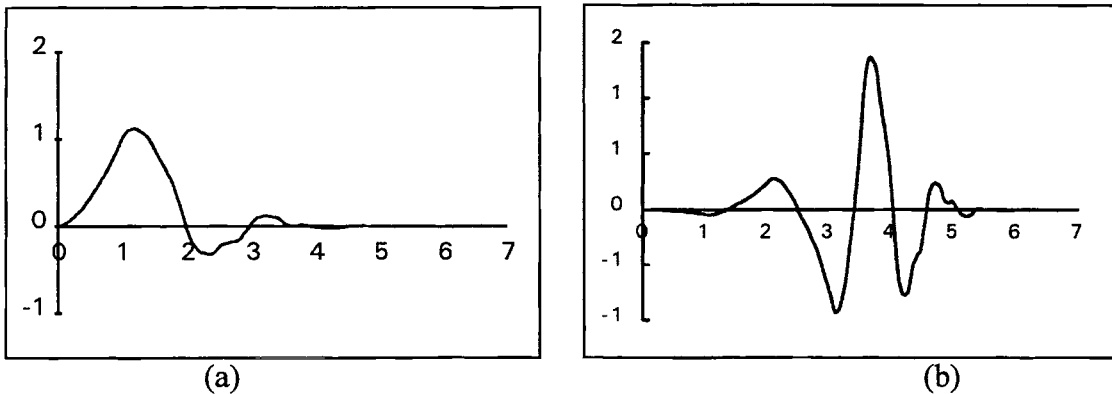


Figure 3: (a) Fourth order Daubechies family scaling function and (b) wavelet

Wavelet transforms provide variable frequency analysis capability instead of constant frequency analysis as in Fourier transforms [Strang, 1993]. The analysis frequency can be varied on a logarithmic scale as shown in Figure 4. Since time and frequency are inversely related, time resolution improves at higher frequencies. Two closely spaced impulses in a real time representation of the signal can be distinguished by a wavelet decomposition.

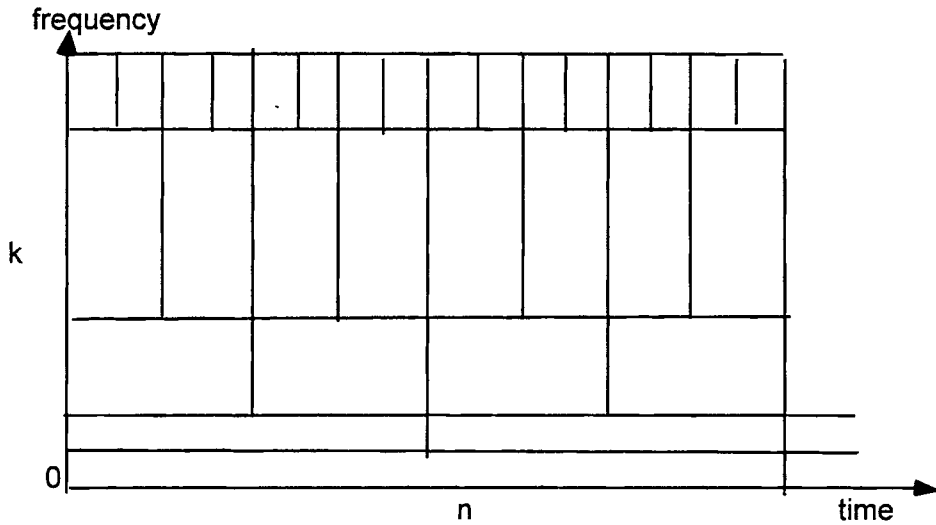


Figure 4: Wavelet transform on a time frequency scale

A comparison of a Fourier decomposition of a signal and a wavelet decomposition of the signal can be seen in Figure 5. The time domain representation of the Fourier transform provides a poor trend pattern representation of the original signal. Its wavelet counterpart on the other hand, provides an excellent trend pattern representation of the original signal. This representation is a replica of the original signal, but on a coarser scale. The second part of the wavelet decomposition contains signal details present in the original signal but lost in the coarse representation. It can be inferred that wavelet transforms provide better time-frequency localization than Fourier transforms.

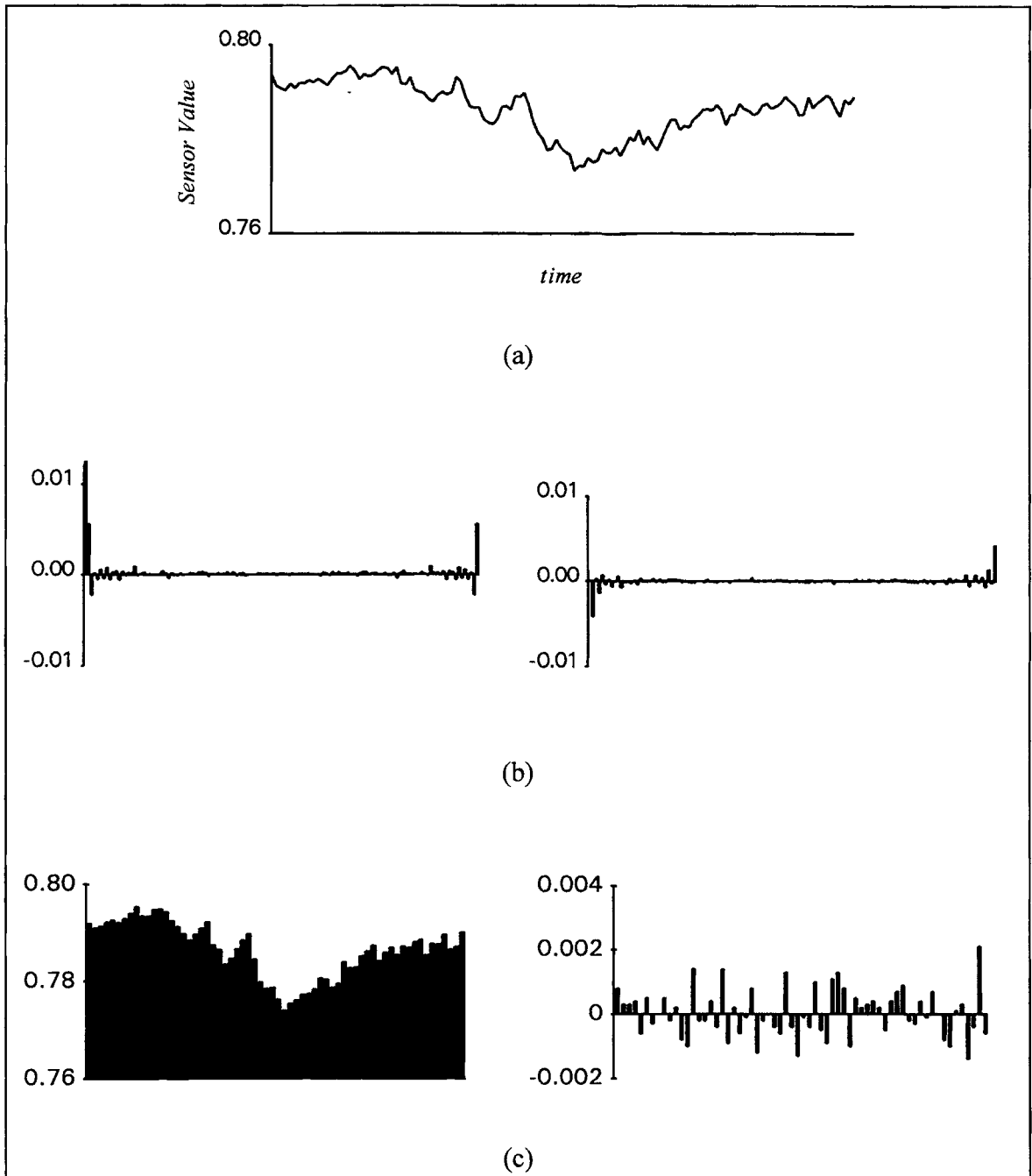


Figure 5: Comparison of Fourier decomposition and wavelet decomposition (a) original signal, (b) Fourier decomposition and (c) wavelet decomposition down one level using the third order Daubechies family.

This chapter introduced two important signal processing techniques. Fourier transforms were described, and their shortcomings were discussed. Fourier transforms work well for stationary signals but not for process signals which are generally not stationary. Wavelet transforms were introduced and their advantages over Fourier transforms were outlined. The next chapter deals with wavelet transforms in greater detail.

## CHAPTER III

### WAVELET TRANSFORMS

#### Introduction

Though wavelet transforms are relatively simple to implement, the mathematics are somewhat complex. This chapter discusses the mathematics of wavelet transforms. The general methodology is discussed, and the Daubechies wavelet family is specifically illustrated [Cohen *et al.*, 1992a; Daubechies, 1992; Daubechies, 1988]. The finer mathematical aspects of multi-resolution analysis are discussed as well as various methods of applying wavelet transforms for multi-resolution analysis. The first subject presented is the dilation equations that constitute the mother functions of both scaling functions and wavelets. Computation of the scaling function and wavelet coefficients is discussed, and the actual synthesis of scaling functions and wavelets is described.

#### Dilation Equations

Scaling functions and wavelets are represented by special types of equations called *dilation equations* [Daubechies, 1992; Daubechies and Lagarias, 1992a; Daubechies and Lagarias, 1992b; Strang, 1989]. The general form is

$$\eta(t) = \sum_k l_k \eta(mt - k) \tag{7}$$

Here,  $l$  is a vector of dilation function coefficients which represents the impulse response of the filter associated with the dilation equation. Consequently the  $l_k$ 's are referred to as the filter coefficients.

The general equation for the scaling function is

$$\varphi(t) = \sum_k c_k \varphi(2^j t - k), \quad (8)$$

where  $c_k$  is the scaling function coefficient. Similarly the wavelet equation is given by

$$\psi(t) = \sum_k d_k \varphi(2^j t - k). \quad (9)$$

where  $d_k$  is the wavelet coefficient.

Note that the scaling functions are expressed as a sum of dilations and translations of the function. Wavelets are defined as functions of the scaling functions, because the decomposition basis functions have to be interdependent.

In equation (7), the term  $m$  provides the ability to dilate depending on the analysis level. Frequency localization is thus obtained. Hence,  $m$  is called the *dilation coefficient*. The function constricts for high frequencies, and dilates to capture lower frequencies. Figure 6 illustrates the dilations and translations of a wavelet. As the level of analysis increases, the functions dilate and span a wider frequency range. During analysis, frequency is gradually sliced in a logarithmic fashion. When  $m$  equals 2, the dilation is binary.

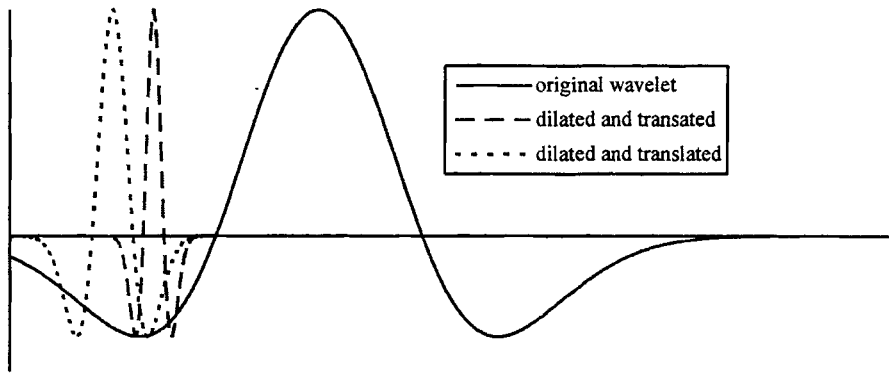


Figure 6: Illustration of a wavelet at different dilations and translations.

The other parameter,  $k$ , is the *translation coefficient* that provides translation in time and thus time localization. This translating coefficient can assume any range of values, though a finite range is generally adopted for computational ease.

Together these parameters provide the necessary time-frequency localization, the most attractive feature of the wavelet method. Generally translations are dyadic. This means that signal sampling after wavelet transform is dyadic, and every alternate decomposition coefficient is sufficient to obtain perfect reconstruction. A uniform sampling grid is maintained in a dyadic wavelet transform [Daubechies, 1990; Oslen and Seip, 1992; Walter, 1992]. Figure 7 shows a sampling grid for wavelet transforms.

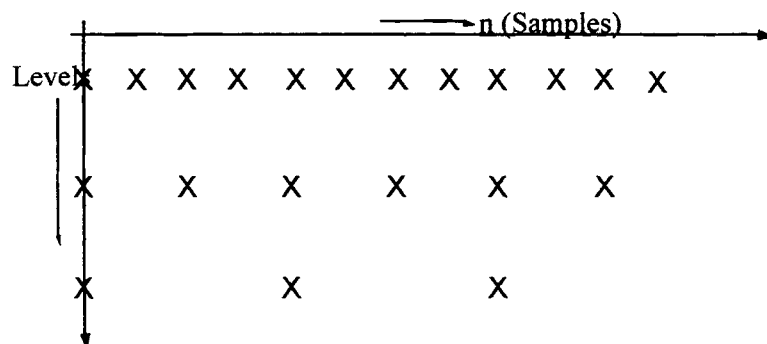


Figure 7: The dyadic sampling of a wavelet grid.



It can be seen that the number of coefficients at any level is half the number of coefficients at the previous level.

Wavelets provide the ability to analyze a signal at multiple resolutions. To resolve the finer details, the resolution is increased. Similarly, when resolution is gradually decreased, the object becomes more and more blurred [Cohen *et al.*, 1992b; Daubechies, 1991; Mallat, 1989a; Mallat, 1989b; Mallat, 1989c]. The coefficients from a wavelet analysis are representative of the original signal, *but across different resolution levels*.

Since a variety of scaling functions and wavelets are possible, we retain the liberty to experiment with different basis functions and to use the decomposition that best suits our needs. The different types of wavelets come about from the fact that in equation (7),  $\eta$  can be different functions and  $k$  can take on different values.

A variety of wavelets [Battle, 1987; Chui, 1992; Chui and Wang, 1991; Chui and Wang, 1992; Cohen *et al.*, 1992a; Daubechies, 1992; Daubechies, 1993; Lemarie, 1990; Lemarie, 1988; Meyer, 1985] can be constructed depending on conditions imposed during their construction. Wavelets are broadly classified into *families*, based on their nature. These families of wavelets are further sub-divided into *orders*, depending on the order of filters, i.e. the filter lengths. Similar to the sines and cosines, wavelets with infinite support can be defined. Recent advances in wavelet technology have led to the development of finitely supported wavelets. Finite length wavelets are advantageous in computational ease over their infinitely supported counterparts, but cause translation variance. Some common wavelet families (Figure 8) are:

- The Daubechies family [Daubechies, 1988] and coiflets [Daubechies, 1992];
- The Battle-Lemarie family [Battle, 1987; Lemarie, 1988];
- The Meyer family [Meyer, 1985];
- Biorthogonal wavelet [Cohen *et al.*, 1992a];

- Wavelets from Cardinal Splines by Chui [Chui, 1992a; Chui and Wang, 1991; Chui and Wang, 1992; Chui and Wang, 1993].

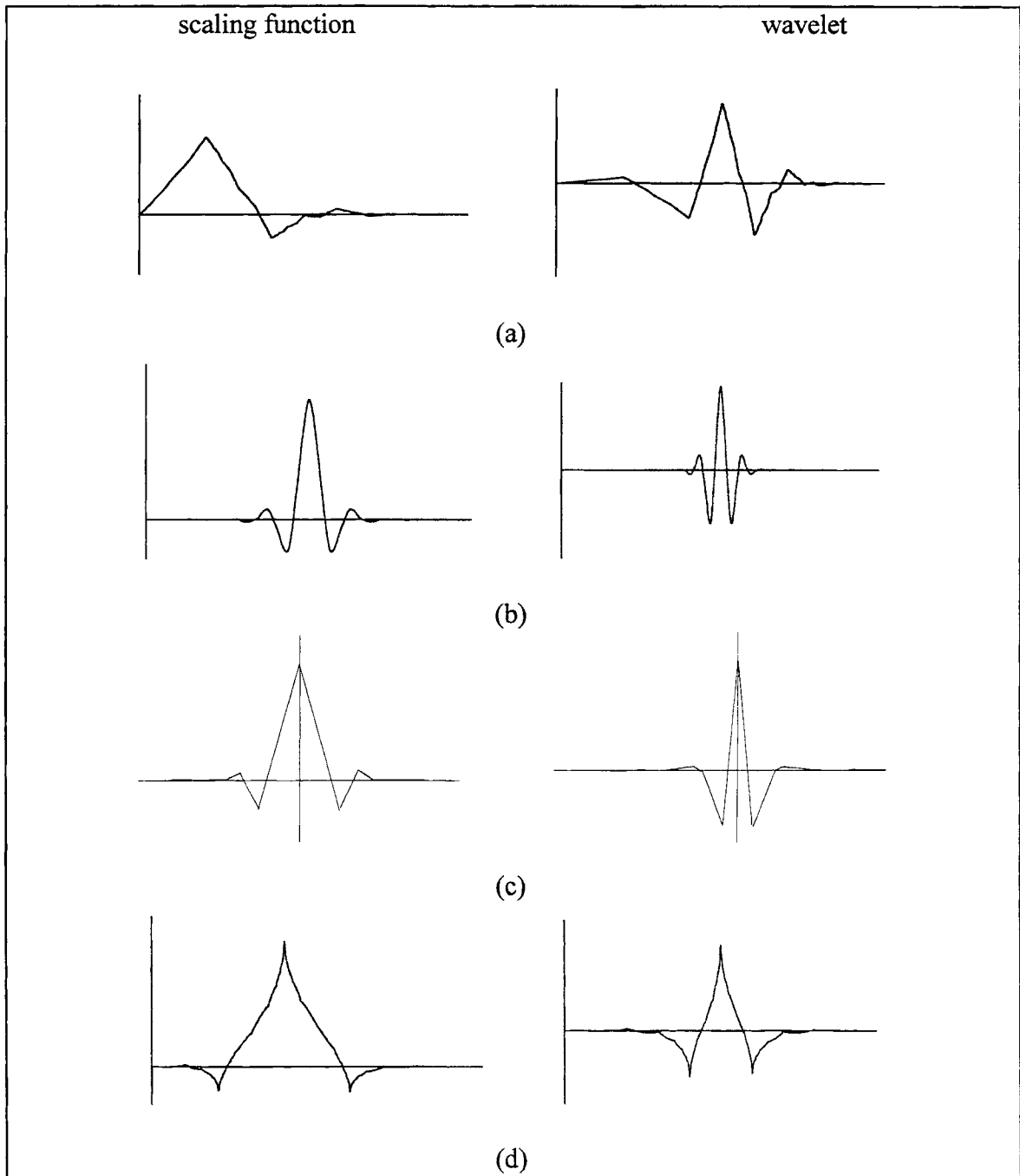


Figure 8: Figure showing some wavelet families, (a) the Daubechies family, (b) biorthogonal wavelets, (c) Battle-Lemarie wavelet and (d) coiflets.

## Wavelet Construction

Before we delve into the actual construction of wavelets, a few terms are defined to facilitate easier understanding of this topic.

**Orthogonality:** A function  $\phi(t)$  is said to be orthogonal if the following relationship is satisfied;

$$\int_a^b \phi_j(t) \phi_k(t) dt = \begin{cases} 0 & j \neq k \\ c & j = k \end{cases} \quad (10)$$

where “ $c$ ” is a constant. When  $c$  is unity, the function is both orthogonal and normalized, i.e., it is *orthonormal*.

In wavelet construction the first step involves computation of the scaling function coefficients in equation (8), the wavelet coefficients in equations (9), and, finally, the actual scaling function and wavelet function.

**Computing the scaling function and wavelet coefficients:** We consider the simplest form of wavelets, called the Haar wavelets.

### Case 1: The Haar case

The Haar wavelet is constructed from the simple box function shown in Figure 9.

The scaling function is a simple box function.

$$\varphi(t) = \begin{cases} 1 & 0 \leq t \leq 1 \\ 0 & \text{otherwise} \end{cases} \quad (11)$$

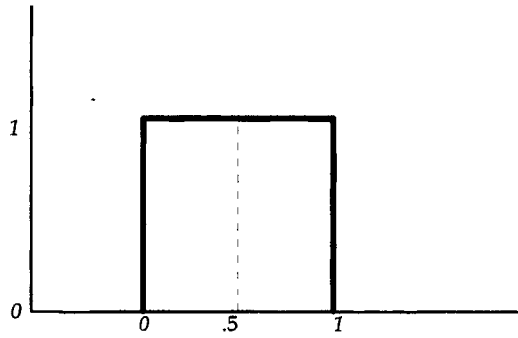


Figure 9: The box function.

This satisfies the dilation equation

$$\varphi(t) = c_0\varphi(2t) + c_1\varphi(2t - 1). \quad (12)$$

Comparing equation (8) with equation (12) gives  $c_0=1$ ,  $c_1=1$ . These are the scaling function coefficients for the Haar wavelet. In this case, the box function is a sum of two half sized boxes, both of uniform dilation. The difference between them is that one box is translated by a unit value. Since the box function is defined by two non-zero coefficients, it is called a filter of length two.

The wavelet corresponding to the box like scaling function in Figure 9 is depicted below along with a dilated version and a dilated and translated version.

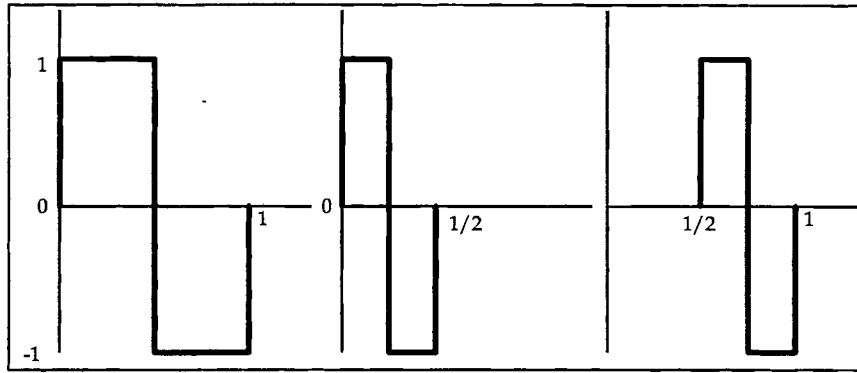


Figure 10: The Haar wavelet  $\psi(t)$  and dilated and translated versions,  $\psi(2t)$ ,  $\psi(2t-1)$ .

The Haar wavelet is given by

$$\psi(t) = d_0\varphi(2t) + d_1\varphi(2t-1), \quad (13)$$

where  $d_0 = 1, d_1 = -1$ . It can also be defined as

$$\psi(t) = \begin{cases} 1, & 0 \leq t < 1/2 \\ -1, & 1/2 \leq t \leq 1 \\ 0, & \text{otherwise} \end{cases} \quad (14)$$

Case 2: A linear spline case:

This example is a wavelet constructed from the simple hat function shown in Figure

11

$$\varphi(t) = \begin{cases} t, & 0 \leq t \leq 1 \\ 2-t, & 1 \leq t \leq 2 \\ 0, & \text{otherwise} \end{cases} \quad (15)$$

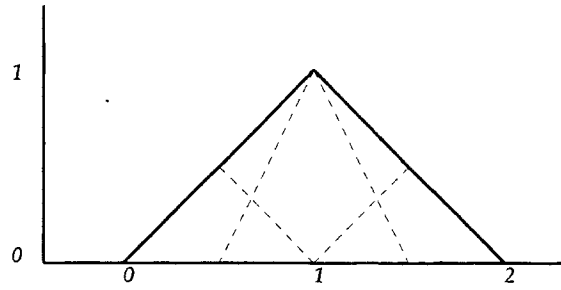


Figure 10: The hat function.

This satisfies

$$\varphi(t) = c_0\varphi(2t) + c_1\varphi(2t-1) + c_2\varphi(2t-2). \quad (16)$$

Equation (16) is satisfied for  $c_0=c_2=1/2$ ,  $c_1=1$ . In this case the scaling function is the sum of three dilated and translated versions. Thus, a variety of combinations of dilated and translated versions of these functions can be used to generate wavelets starting from different basis functions. This is possible, provided the basis functions meet certain requirements documented in the following sections.

The wavelet for the hat function is shown in Figure 12. This wavelet is expressed in

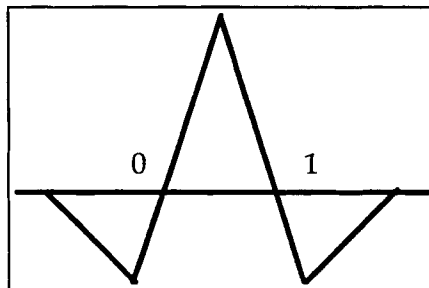


Figure 12: Wavelet associated with the Hat function

the form of a dilation equation as follows:

$$\psi(t) = d_0\phi(2t) + d_1\phi(2t-1) + d_2\phi(2t+1) \quad (17)$$

where  $d_0=1, d_1=d_2=-1/2$ .

In case 2, the scaling function is composed of combinations of polynomials that are piecewise linear; case 1 is satisfied using simple constants. Piecewise linear polynomials are not effective at approximating [Rice, 1964] stochastic signals like sensor signals. Higher order polynomials can also be used [Daubechies, 1988] and are better for approximating these kinds of behavior. Polynomials that provide both orthogonality and compact support are preferred over other kinds of approximating functions. This was not achieved until Daubechies constructed such functions [Daubechies, 1988]. The beauty of Daubechies wavelets is that they are not only orthogonal but are compactly supported as well. It was previously believed that orthogonality could only be achieved at the expense of compact support. The next section extends the procedure for the Daubechies family.

**The Daubechies Family:** Wavelet construction is actually preferred in the frequency domain because dilation and translation parameters are more easily handled in the frequency domain than in the time domain. In the general methodology [Chui, 1992a; Daubechies, 1992; Daubechies, 1993; Strichartz, 1993], translates of the scaling function are approximated by a polynomial. The coefficients of the polynomial are the scaling function coefficients  $c_k$ 's.

Depending on the nature of the wavelet desired, constraints are imposed during the construction of the scaling function. For instance, the orthonormality condition imposed is

$$\int \phi(t) dt = 1 \quad (18)$$

and for orthogonality,

$$\int \psi(t) dt = 0. \quad (19)$$

Orthogonality is necessary for perfect signal reconstruction.

A limit is imposed on the number of finite non-zero  $c_k$  to ensure that the scaling function and wavelet are compactly supported or span a finite range. Support is defined as the span of the scaling function or the wavelet; i.e. the spread or expanse over which the function has a non-zero value.

Once the scaling function is constructed, the wavelet is then constructed from the dilation equation (9). Constraints imposed on scaling functions and wavelets are actually constraints on their respective coefficients, as is evident from the equations below. Integrating equation (8) and comparing the orthonormality condition (equation 18)

$$\int \phi(t) dt = \int \sum c_k \phi(2t - k) dt = 1$$

and

$$\sum c_k = 2. \quad (20)$$

Similarly, integrating equation (9) with the orthogonal condition described by equation 19

$$\int \psi(t) dt = \int \sum d_k \phi(2t - k) dt = 0$$

or,

$$\sum d_k = 0 \quad (21)$$

The condition for a set of wavelet functions to be orthogonal is that the sum of its scaling function coefficients should be two (from equation (20)). For the wavelet functions to be orthonormal as well, the sum of the wavelet coefficients should be zero.



There is a special relationship between the  $c_k$  and  $d_k$  when the scaling function and wavelet function are Quadrature Mirror Filters (QMF's) of each other [Akansu *et al.*, 1993; Cohen *et al.*, 1992a; Daubechies, 1988]. This relationship is given by

$$d_k = (-1)^{1-k} c_{1-k}. \quad (22)$$

Simply stated, the wavelet coefficients are obtained from the scaling function coefficients by reversing the order and changing the signs on every alternate coefficient. This way, we need not calculate the wavelet coefficients (the  $d_k$ 's) separately. They can be obtained directly from the scaling function coefficients ( $c_k$ 's).

This procedure is illustrated further by an example [Daubechies, 1988]. The construction of the Daubechies family of compactly supported orthonormal wavelets is briefly discussed in the following paragraphs. Only an abstract of the construction method is discussed in this work. The full treatment of this topic can be obtained from [Akansu and Haddad, 1993; Chui, 1992a; Daubechies, 1992; Daubechies, 1993; Haykin, 1991; Strang, 1989]. The conditions imposed for the construction of the Daubechies family of wavelets are that the scaling function has  $2N$  coefficients and lies supported between  $0$  and  $2N-1$ , where  $N$  is the order of the wavelet within the family. This means that the coefficients, other than those lying in the region between  $0$  and  $2N-1$ , are zero in value. This gives rise to the following condition:

$$c_n = 0 \text{ for } n < 0 \text{ or } n > 2N-1 \quad (23)$$

Also, they form an orthonormal family of wavelets. Since there are only a finite number of coefficients, equations (20) and (21) yield

$$\begin{aligned}\sum_{k=0}^{2N-1} c_k &= 2 \\ \sum_{k=0}^{2N-1} d_k &= 0.\end{aligned}\tag{24}$$

As mentioned previously, actual construction of scaling functions is performed in the frequency domain. The Fourier transform of a function  $f(x)$  is defined as

$$\hat{f}(\xi) = \frac{1}{\sqrt{2\pi}} \int e^{-i\xi x} f(x) dx.\tag{25}$$

Note that this is the continuous Fourier transform. The previously described equation (5) is the discrete version of this transform.

The Fourier transform of the scaling function is

$$\frac{1}{\sqrt{2\pi}} \int e^{-i\xi x} \varphi(x) dx = \frac{1}{\sqrt{2\pi}} \sum_k c_k \int e^{-i\xi x} \varphi(2x - k) dx.$$

Simplifying,

$$\hat{\varphi}(\xi) = \frac{1}{2} \sum_k c_k e^{-ik\xi/2} \hat{\varphi}\left(\frac{\xi}{2}\right).\tag{26}$$

This equation can now be expressed as function of another simple equation. Define

$$m_0(\xi) = \frac{1}{2} \sum_k c_k e^{-ik\xi/2},\tag{27}$$

then equation (26) can be expressed as

$$\hat{\varphi}(\xi) = m_0\left(\frac{\xi}{2}\right) \hat{\varphi}\left(\frac{\xi}{2}\right).\tag{28}$$

Also, equation (28) can be further extended as

$$\hat{\phi}(\xi) = m_0\left(\frac{\xi}{2}\right)\hat{\phi}\left(\frac{\xi}{2}\right) = m_0\left(\frac{\xi}{2}\right)m_0\left(\frac{\xi}{4}\right)\hat{\phi}\left(\frac{\xi}{4}\right) \cdots = \prod_{j=1}^{\infty} m_0\left(\frac{\xi}{2^j}\right). \quad (29)$$

Equation (29) indicates that the translates of  $\phi(t)$  can be approximated by an infinite length polynomial. For the Daubechies case, however, approximation is attempted using a finite length polynomial. Obviously, not all finite length polynomials meet the orthonormality requirements. Only special types of polynomials can possibly satisfy all the requirements. This polynomial should also provide the best approximation for the desired scaling function. From equation (27) it can be seen that the coefficients of the polynomial directly yield the scaling function coefficients. Since real coefficients are preferred, the polynomial in equation (27) is a cosine polynomial, the reason being that the polynomial in equation (27) is expressed as a function of  $e^{-i\xi}$  whose real part is the cosine part. The proof that this polynomial is periodic is given in Appendix A. Using  $z=e^{-i\xi}$ , the polynomial is transformed into a function of  $z$ .

The polynomial in equation (27) is subsequently defined as

$$m_0\left(\frac{\xi}{2}\right) = P(z) = \left(\frac{1+z}{2}\right)^N E(z) \quad . \quad (30)$$

Here  $E(z)$  is the cosine polynomial and constitutes the real part of the polynomial in equation (27). Thus only real coefficients will be generated. The periodicity of  $P(z)$  causes it to satisfy equation (31)

$$\left|m_0\left(\frac{\xi}{2}\right)\right|^2 + \left|m_0\left(\frac{\xi}{2} + \pi\right)\right|^2 = |P(z)|^2 + |P(-z)|^2 = 1. \quad (31)$$

The importance of this equation is our attempt to generate functions that are as symmetric as possible.

The general solution to equation (31) is given by

$$|E(z)|^2 = \sum_{k=0}^{N-1} \binom{N-1+k}{k} \left(\sin \frac{\xi}{2}\right)^{2k} + \left(\sin \frac{\xi}{2}\right)^{2N} \tau_0\left(\frac{\cos \xi}{2}\right). \quad (32)$$

From equation (32), using a technique called spectral factorization [Chui, 1992a; Daubechies, 1988]),  $|E(z)|$ , the absolute value of the polynomial is substituted in equation (30) which gives the coefficients for the scaling function for the Daubechies Family. From the QMF relationship described by equation (22), the wavelet coefficients are computed.

The construction can be summarized as follows :

- The order of the wavelet  $N$  is decided and the polynomial in equation (32) is synthesized.
- The polynomial is spectral factorized and the “square root” of the polynomial is calculated.
- The polynomial from step (2) is multiplied with another binomial polynomial as in equation (30) to make the resultant polynomial as regular as possible. Binomial polynomials are always symmetric.
- A polynomial of order  $2N-1$  results from step (2). Normalization of these coefficients according to equation (27) gives the scaling function coefficients for the  $N^{\text{th}}$  order Daubechies family of wavelets.
- The wavelet coefficients are calculated from the relationship in equation (22).

A more detailed explanation of this procedure is described in Appendix A. Also illustrated in Appendix A is the procedure for calculating the scaling function and

wavelet coefficients for the second order Daubechies family. The next section describes construction of scaling functions and wavelets from their respective coefficients.

**Construction of the scaling function and wavelet:** Having generated the scaling function coefficients and wavelet coefficients, we proceed to calculate the actual function values using a method adopted from Gilbert Strang's classic article [Strang, 1989].

Scaling function values are calculated at integer points. This is done by constructing a matrix  $M_{ij} = c_{2i-j-1}$ . The left eigenvector for  $\lambda = 1$  gives the value of the scaling function at the integer points.

Construction of the scaling function and wavelet for the second order Daubechies family is described below.

By definition, the following equality holds for the Daubechies second order family:

$$\varphi(t) = 0 \quad \text{for } t \leq 0 \text{ and } t \geq 3. \quad (33a)$$

The value of the scaling function at  $t=1$  and  $t=2$  must be evaluated. For  $t=1$  and  $t=2$  in equation (8),

$$\varphi(1) = c_0\varphi(2) + c_1\varphi(1) \quad (33b)$$

$$\varphi(2) = c_2\varphi(2) + c_3\varphi(1) \quad (33c)$$

Solving these two equations simultaneously is identical to solving the matrix

$$\begin{bmatrix} \varphi(0) \\ \varphi(1) \\ \varphi(2) \\ \varphi(3) \end{bmatrix} = \begin{bmatrix} c_0 & 0 & 0 & 0 \\ c_2 & c_1 & c_0 & 0 \\ 0 & c_3 & c_2 & c_1 \\ 0 & 0 & 0 & c_3 \end{bmatrix} \begin{bmatrix} \varphi(0) \\ \varphi(1) \\ \varphi(2) \\ \varphi(3) \end{bmatrix}, \quad (33d)$$

equation (8). Inserting zeros between the known values of the scaling function, the resultant vector is  $[\varphi(0) \ 0 \ \varphi(1) \ 0 \ \varphi(2) \ 0 \ \varphi(3)]$ . This vector is convolved with the scaling function coefficients. The resultant vector contains the values  $[\varphi(0) \ \varphi(0.5) \ \varphi(1) \ \varphi(1.5) \ \varphi(2) \ \varphi(2.5) \ \varphi(3)]$ .

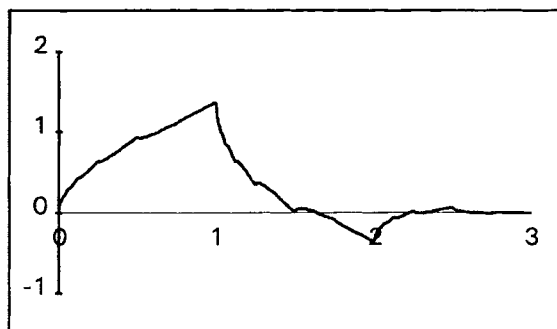
This operation can be repeated to calculate the scaling function values at any number of intermediate points.

The wavelet values are computed in the same manner. To compute the wavelet values at  $n$  points, the scaling function values at only half the number of points are needed, i.e., the values of scaling function at only  $n/2$  points are needed. Zeros are inserted between each value of scaling function and convolved with the wavelet coefficients. The first  $n$  points of the convolution product are retained and provide the values of the wavelet at the desired points.

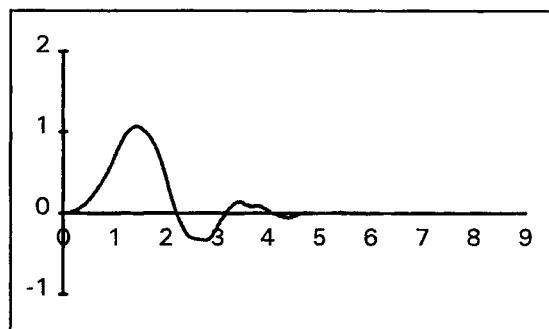
Sample coefficients are shown in Table I. Figures 13 and 14 show some Daubechies family scaling functions and their corresponding wavelets.

Scaling function coefficients for the Daubechies family. N is the order of the wavelet		
N=2	N=7	N=9
0.48296291314453	0.07785205408501	0.03807794736391
0.83651630373781	0.39653931948193	0.24383467461279
0.22414386804201	0.72913209084625	0.60482312369057
-0.12940952255126	0.46978228740519	0.65728807805169
N=3	-0.14390600392858	0.13319738582482
0.33267055295008	-0.22403618499389	-0.29327378327973
0.80689150931109	0.07130921926683	-0.09684078322325
0.45987750211849	0.08061260915109	0.14854074933814
-0.13501102001025	-0.03802993693502	0.03072568147931
-0.08544127388203	-0.01657454163067	-0.06763282906141
0.03522629188571	0.01255099855610	0.00025094711483
N=4	0.00042957797292	0.02236166212370
0.23037781330890	-0.00180164070405	-0.00472320475776
0.71484657055292	0.00035371379997	-0.00428150368247
0.63088076792986	N=8	0.00184764688306
-0.02798376941686	0.05441584224311	0.00023038576352
-0.18703481171909	0.31287159091434	-0.00025196318894
0.03084138183556	0.67563073629737	0.00003934732032
0.03288301166689	0.58535468365426	N=10
-0.01059740178507	-0.01582910525641	0.02667005790061
N=5	-0.28401554296164	0.18817680007804
0.16010239797420	0.00047248457388	0.52720118893260
0.60382926979720	0.12874742662049	0.68845903945440
0.72430852843778	-0.01736930100181	0.28117234366010
0.13842814590132	-0.04408825393080	-0.24984642432883
-0.24229488706639	0.01398102791740	-0.19594627437823
-0.03224486958464	0.00874609404741	0.12736934033608
0.07757149384005	-0.00487035299345	0.09305736460388
-0.00624149021280	-0.00039174037338	-0.07139414716645
-0.01258075199908	0.00067544940645	-0.02945753682182
0.00333572528547	-0.00011747678412	0.03321267405949
N=6		0.00360655356698
0.11154074335011		-0.01073317548335
0.49462389039846		0.00139535174706
0.75113390802111		0.00199240529519
0.31525035170919		-0.00068585669496
-0.22626469396545		-0.00011646685513
-0.12976686756727		0.00009358867032
0.09750160558732		-0.00001326420289
0.02752286553031		
-0.03158203931749		
0.00055384220116		
0.00477725751095		
-0.00107730108531		

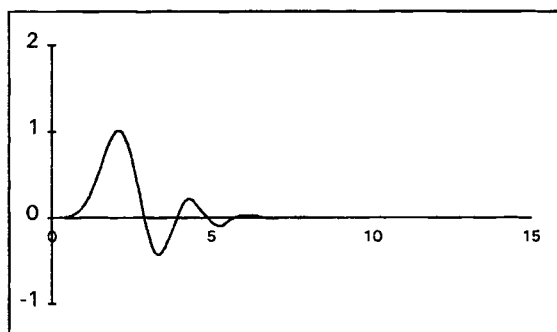
Table I: Scaling function coefficients for the Daubechies family of wavelets (Daubechies 1988).



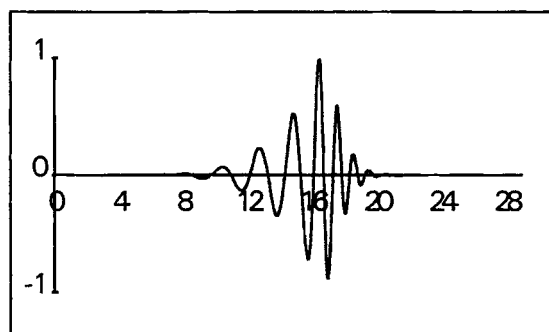
(a)



(b)



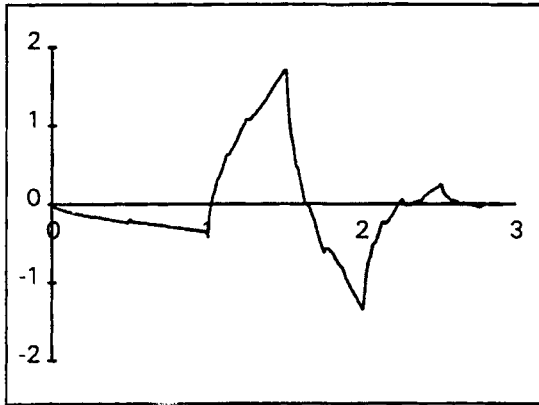
(c)



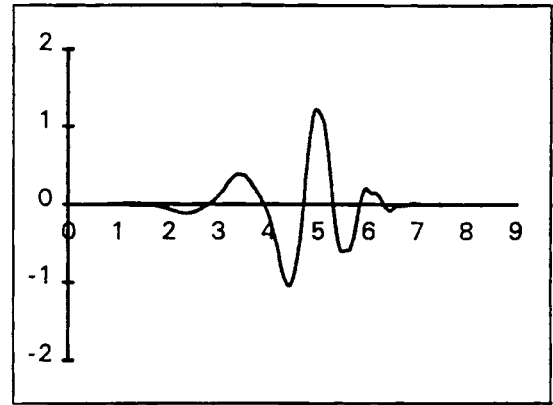
(d)

Figure 13: Scaling functions associated with the Daubechies wavelets for (a) order = 2, (b) order = 5, (c) order = 8 and (d) order = 15.

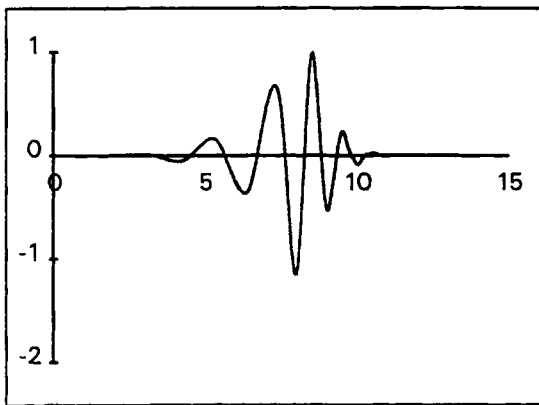




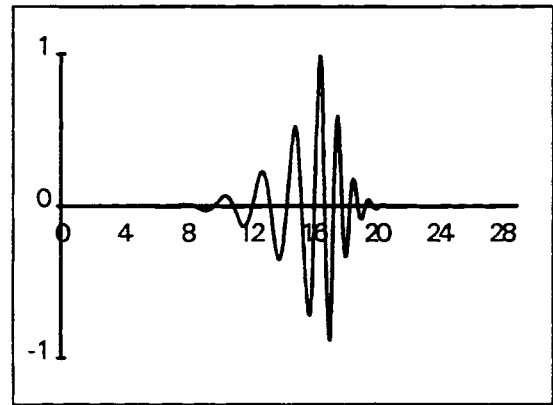
(a)



(b)



(c)



(d)

Figure 14: Daubechies wavelets for (a) order = 2, (b) order = 5, (c) order = 8 and (d) order = 15.

**Computing the decomposition coefficients:** Signal filtering is mathematically performed using convolution. Signals are convolved with the filter coefficients (in this case, with the scaling function and the wavelet coefficients) and the resultant product signal dyadically sampled. If  $f$  is the process signal,  $H$  and  $G$  the high pass filters (scaling functions) and the bandpass filters (wavelets) respectively, then the signal is decomposed as follows.

$$\text{Blurred Signal} = H * f$$

$$\text{Detail Signal} = G * f$$

where “\*” represents the convolution operation followed by downsampling in which every alternate value is retained. The detail signal contains information in the original signal which is missing in the blurred signal. There is no loss of information if the transformation is orthogonal. The original signal can be reconstructed from any level by simply reversing this operation.

$$H' \wedge (\text{Blurred Signal}) + G' \wedge (\text{Detail Signal}) = \text{Original Signal}.$$

$H'$  and  $G'$  are transpose of  $H$  and  $G$ . In this step, however, the “ $\wedge$ ” represents an upsampling operation. Upsampling is a doubling of the signal length by insertion of zeros between each value and convolving with the filter coefficients as described earlier. Figure 15 best represents this whole procedure.

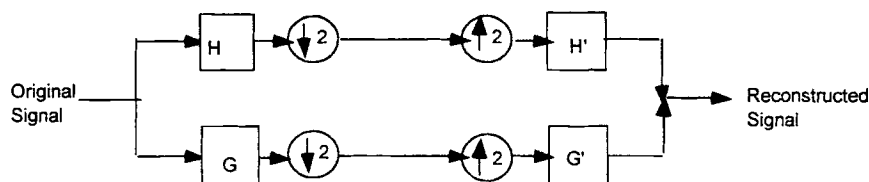


Figure 15: A basic decomposition and reconstruction representation.

Consider a signal  $f$  at its original resolution, having  $n$  samples and whose time domain representation is vector  $a^0$ . At this resolution the elements of the vector  $a^0$  are the sampled values of the signal itself. The decomposition coefficients generated at the first level of decomposition are given by

$$a_j^1 = \frac{1}{2} \sum_k a_k^0 c_{2j-k} \quad j = 1, \dots, \frac{n}{2}, k = 1, \dots, n \quad (34a)$$

$$b_j^1 = \frac{1}{2} \sum_k a_k^0 d_{2j-k} \quad j = 1, \dots, \frac{n}{2}, k = 1, \dots, n, \quad (34b)$$

where the  $c_k$  and  $d_k$  are the scaling function and wavelet coefficients respectively (computed according to the procedure in the previous section). The  $1/2$ s before the summations are normalization constants. At any level the signal decomposition coefficients  $a$  and  $b$  are computed by recursion from the results at the previous level. The sequence  $a_n^1$  can be considered as an averaged version of the original signal, *but on a scale twice as large*. Equations (34a) and (34b) are equivalent to convolving the signal with the respective filter coefficients and downsampling them by a factor of two. On the other hand, sequence  $b_n^1$  contains the difference in information between the signal  $a_n^1$  and the signal  $a_n^0$ , i.e., the information present in the original signal *but filtered out in the averaged version*.

A sample illustration of this decomposition procedure is provided using the Haar wavelet and a short signal. The Haar family is chosen for simplicity. Consider a signal vector  $a_n^0$  represented by four sampled values  $[a_1 \ a_2 \ a_3 \ a_4]$ . Let the scaling function coefficients be  $[c_0 \ c_1]$  and the wavelet coefficients be  $[d_0 \ d_1]$ . The scaling function and wavelet coefficients are  $[1 \ 1]$  and  $[1 \ -1]$ , respectively. Recursion using equations (34a and 34b) results in

$$a_1^1 = \frac{1}{2}[a_1^0 c_1 + a_2^0 c_0] \quad (34c)$$

$$a_2^1 = \frac{1}{2}[a_3^0 c_1 + a_4^0 c_0] \quad (34d)$$

where  $a^1 = [a_1^1 \ a_2^1]$ . Similarly  $b^1 = [b_1^1 \ b_2^1]$  is calculated using equation (34b).

From the decomposition coefficients, it is possible to reconstruct the signal. The recursion is run in reverse as follows:

$$a_k^0 = \sum_j a_j^1 c_{2j-k} + \sum_j b_j^1 d_{2j-k} \quad k = 1, \dots, n. \quad (35)$$

Consider a signal  $a^0 = [2 \ 4 \ 6 \ 8]$ . From equations (34c) and (34d) we get the decomposition coefficients:

$$\begin{aligned} a_1^1 &= \frac{1}{2}[a_1^0 c_1 + a_2^0 c_0] = \frac{1}{2}[1x2 + 1x4] = 3, \\ a_2^1 &= \frac{1}{2}[a_3^0 c_1 + a_4^0 c_0] = \frac{1}{2}[1x6 + 1x8] = 7, \\ b_1^1 &= \frac{1}{2}[b_1^0 d_1 + b_2^0 d_0] = \frac{1}{2}[1x2 - 1x4] = -1, \text{ and} \\ b_2^1 &= \frac{1}{2}[b_3^0 d_1 + b_4^0 d_0] = \frac{1}{2}[1x6 - 1x8] = -1. \end{aligned}$$

So  $a^1 = [3 \ 7]$  and  $b^1 = [-1 \ -1]$ .

Reconstruction is performed using equation (35),

$$\begin{aligned} a_1^0 &= [1x3 + 0x7] + [1x - 1 + 0x - 1] = 2, \\ a_2^0 &= [1x3 + 0x7] + [-1x - 1 + 0x - 1] = 4, \\ a_3^0 &= [0x3 + 1x7] + [0x - 1 + 1x - 1] = 6, \text{ and} \\ a_4^0 &= [0x3 + 1x7] + [0x - 1 + -1x - 1] = 8 \end{aligned}$$

and provides the original signal  $a^0 = [2 \ 4 \ 6 \ 8]$ .

All these operations can be generalized to handle filters of any order and signals of any number of samples.

**Multi-Resolution Analysis:** The previous example illustrated computing decomposition coefficients for the first level and then reconstructing the signal from those coefficients. However, it is possible to decompose the signal further. Coefficients from the first level of decomposition can be decomposed repeatedly to further smooth the signal.

This method of viewing a signal at multiple resolutions is called the **Multi-Resolution Analysis (MRA)** [Cohen *et al.*, 1992b; Daubechies, 1991; Mallat, 1989a; Mallat, 1989b; Mallat, 1989c]. This method provides an excellent tool for feature extraction and pattern recognition. Compact representation of the trends in the original sensor signal can be obtained from decomposition results many levels down. However, dropping down too many decomposition levels yields an overly smoothed trend, so a optimum level must be selected that gives the most compact representation without sacrificing important trend information. The basic representation of MRA is given in Figure 16.

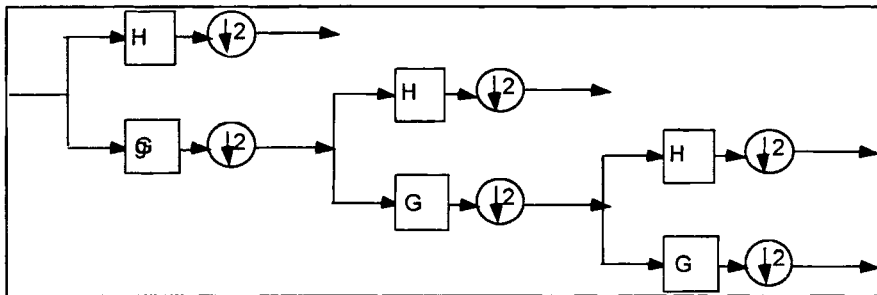


Figure. 16: Depiction of the MRA algorithm.

Figure 17 shows the decomposition of a signal down three levels. It is evident that the signal at any level is the sum of the blurred and detail signals at the previous level.

A wavelet toolbox for analyzing sensor signals was developed during the course of this work here at Oklahoma State University, using MATLAB. Program *daub.m* generates the Daubechies wavelet coefficients for the order specified. File *scale2.m* computes the scaling function and wavelet and plots them. Programs *fwf.m* and *ifwf.m* do the decomposition and reconstruction sequences. All the figures in this chapter were generated using this very user-friendly toolbox.

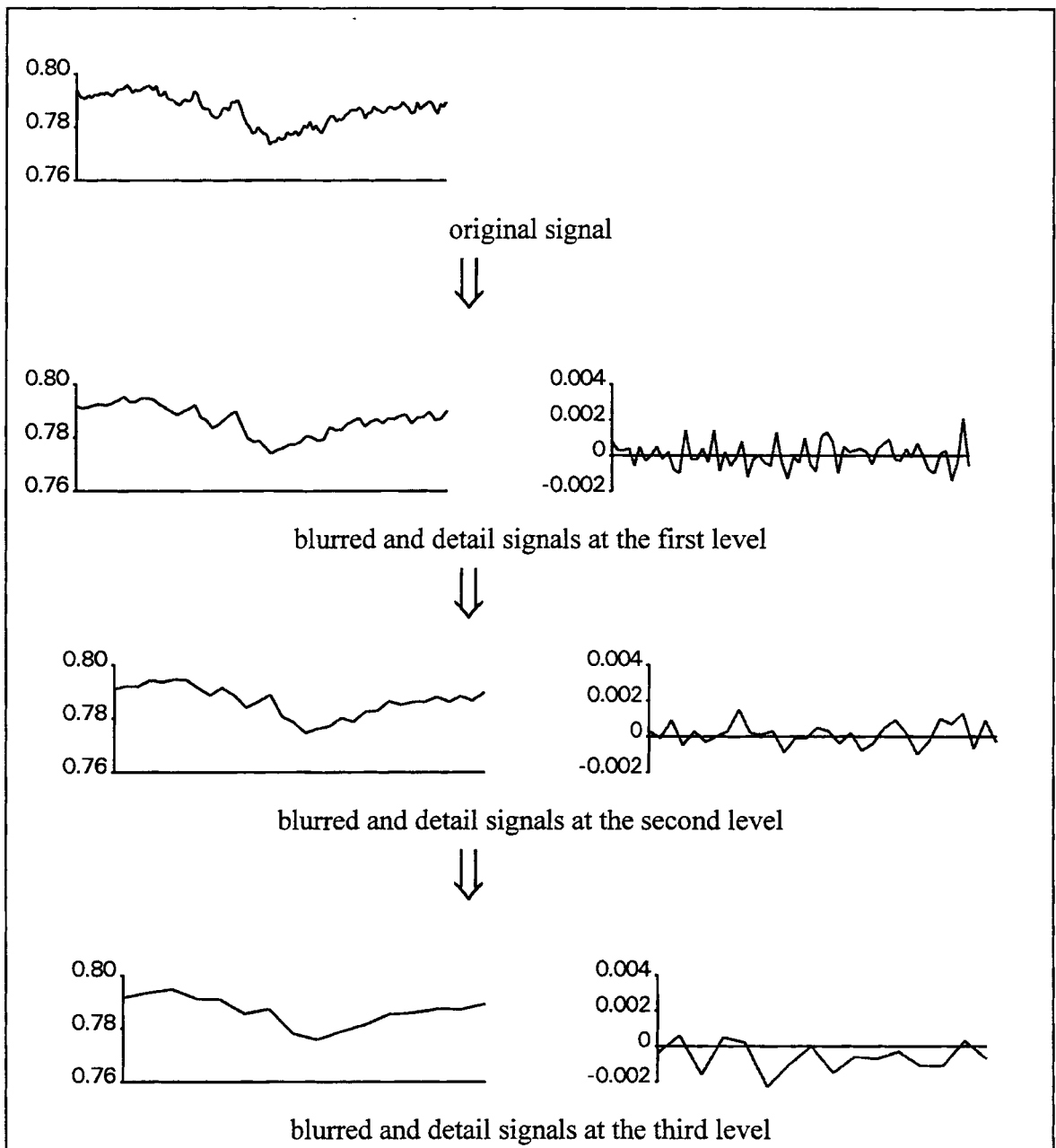


Figure 17: Representation of a signal decomposition up to three levels

## **Chapter Summary**

This chapter addressed the important mathematical aspects of wavelets and wavelet transforms in general and the implementation of wavelet transforms. Emphasis was placed on Daubechies wavelets because that wavelet family was used for the results shown in the next chapter. Not only is this family the most well documented compactly supported wavelet available, but it also exhibits good trend extraction abilities.

The main objective of this chapter was to present wavelets and wavelet transforms in a simplified manner stressing more applied methods and less theoretical details. The next chapter deals with some critical issues in wavelet transforms and their application for trend extraction.



## **CHAPTER IV**

### **SIGNAL EXTENSION**

#### **Need for signal extension for sensor signals from chemical processes**

For computational reasons, process monitoring techniques generally require compact representations of process signals. Raw trend patterns are not preferred for these applications. Therefore, signal processing methods, like wavelet transforms, are used for obtaining a representation more suitable for monitoring purposes. Most signal processing techniques adopt convolution operations for signal analysis and smoothing. An inherent tendency of convolution is to distort finite length signals at the boundaries. For pattern recognition applications, this is unacceptable. It is imperative that signal trends remain unaffected and retain critical features. Signal extension is employed to overcome distortion at the boundaries.

This chapter highlights the inadequacies of common signal extension methods and the development of a new signal extension method.

## Common signal extension methods

Common signal extension methods include circular padding or periodic extension, symmetric extension, extension with zeros, and extension with constant boundary value.

**Circular Extension:** The signal is assumed to be periodic (Figure 18) i.e., the signal is assumed to repeat itself with a period equal to its length.

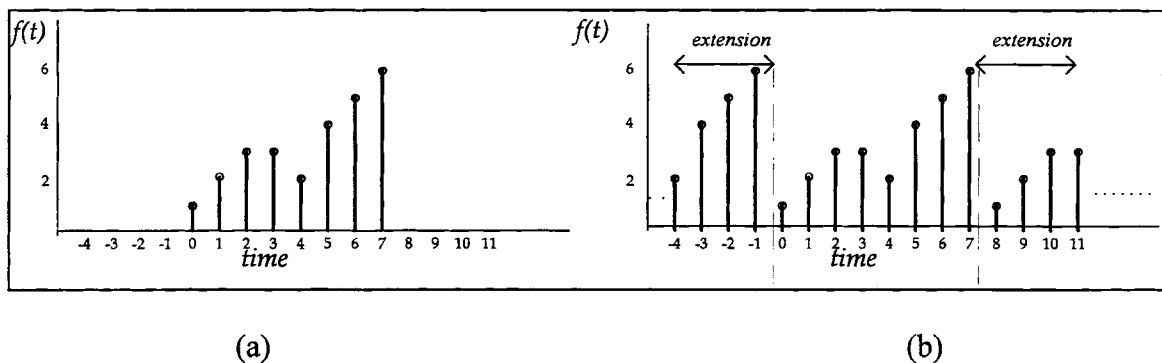


Figure 18: Periodic extension technique, (a) original signal and (b) the extended signal

This method works fine for cases when signals are steady over a period of time. The disadvantage of periodic extension occurs when the points at the extremities of the signal differ significantly as shown in Figure 19. The signal in Figure 19a is decomposed using wavelet transforms and the resultant signal is depicted in Figure 19b. The wavelet decomposition was generated using the sixth order Daubechies wavelet and shows the signal reconstructed from 9<sup>th</sup> decomposition level.

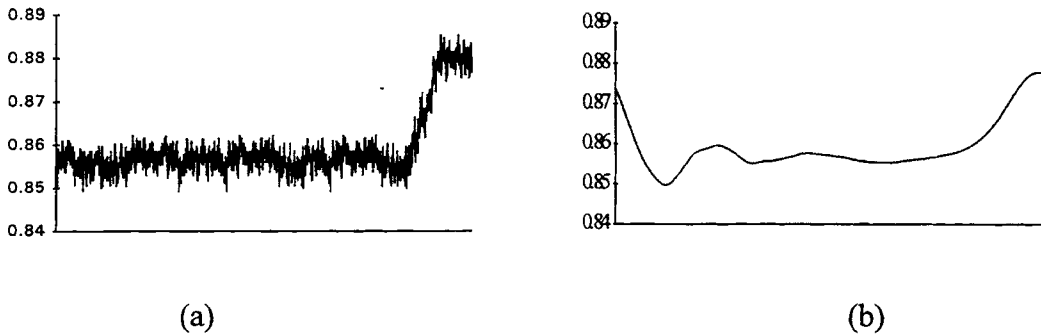


Figure 19: (a) original signal (b) wavelet decomposition using periodic extension.

The periodic extension introduces sharp differences at the boundaries. For instance, in Figure 19, the original signal shows a step change that introduces a significant difference in the sensor value between the two extremities. The inherent nature of the periodic extension averages out signal trends at the boundaries. Therefore, this method is inadequate for our purposes because it seriously distorts trends.

**Symmetric Extension:** Figure 20 depicts a signal that is symmetrically extended. The signal is assumed to be symmetric about the boundary sample on either end.

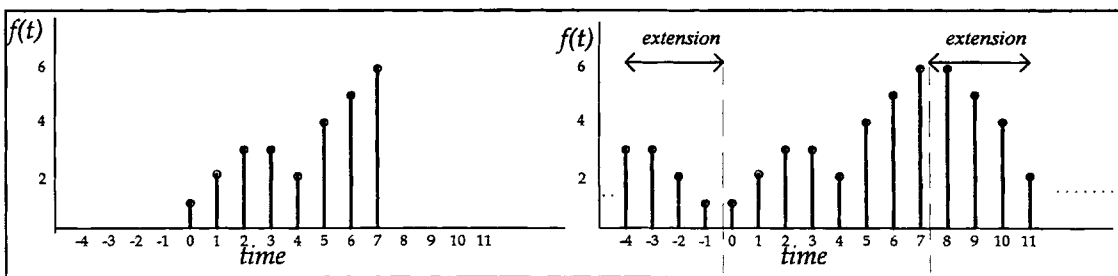


Figure 20: Symmetric extension technique, (a) original signal and (b) the extended signal

Figure 21 depicts a signal with sudden trend changes at the boundaries. The sensor shows a steady value near the boundaries, but at the boundary itself, there is a marked change in the signal behavior.

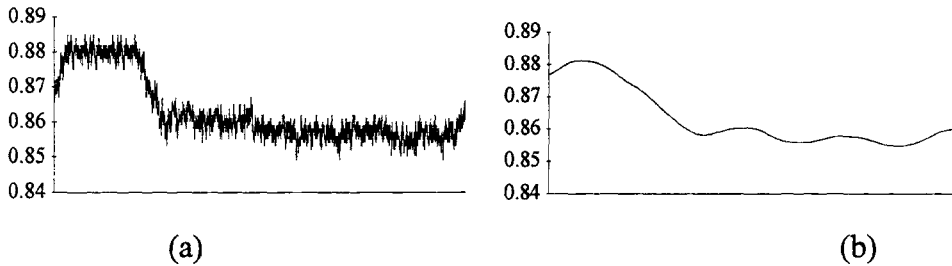


Figure 21: (a) Original signal (b) wavelet decomposition using symmetric extension. Note distortion of trend at the boundaries.

In signals where sharp trends (upward or downward) begin to at the boundary, this signal extension method fails. Symmetric extension flattens the trend at the ends and provides an erroneous representation. This extension procedure is therefore inadequate for wavelet transforms. An interesting observation is that both circular and symmetric extension methods work well for Fourier transforms and other transforms.

**Padding with zeros:** In this signal extension procedure, the signal is extended with zeros as illustrated in Figure 22.

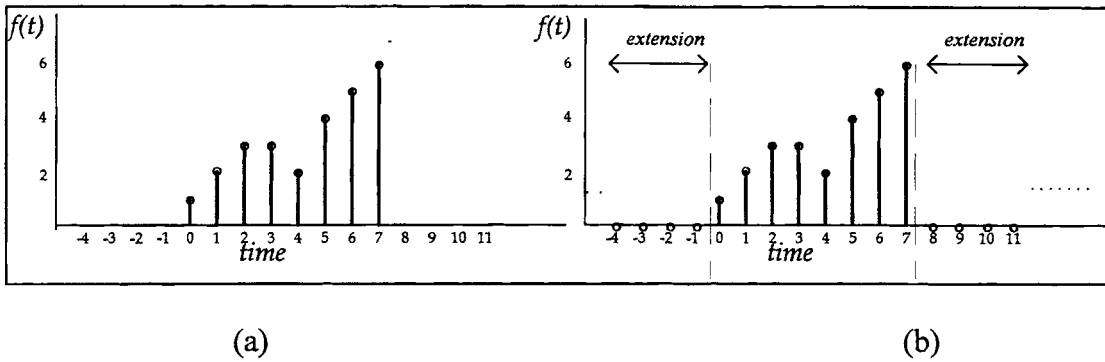


Figure 22: Extension with zeros, (a) original signal and (b) the extended signal

This method fails totally as is illustrated in figure 23.

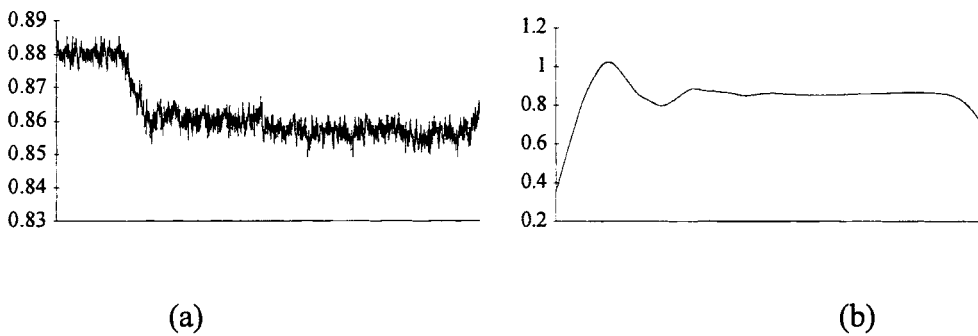
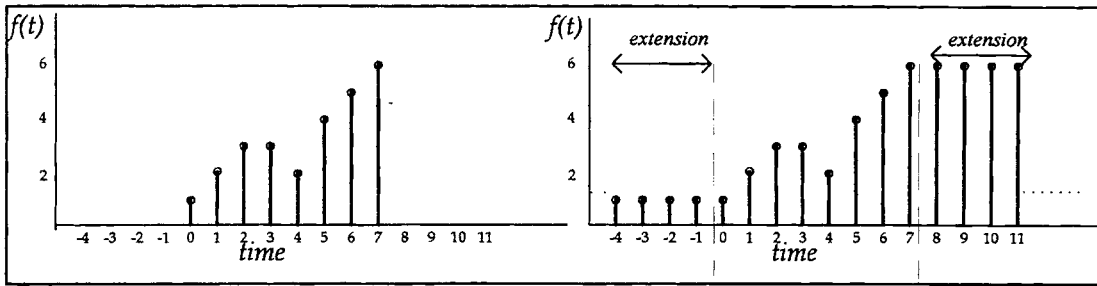


Figure 23: (a) original signal (b) wavelet decomposition using zero padding.  
*The two plots are of different scale to illustrate the extent of distortion of trend at the boundaries.*

It is evident that the zero extension method results in totally misleading trend patterns. The zero extension method is also inadequate for trend retention.

**Padding with a constant value:** This method is similar to the zero extension method, except that the signal is extended to the required length with the boundary value at either end. This technique is illustrated in Figure 24.

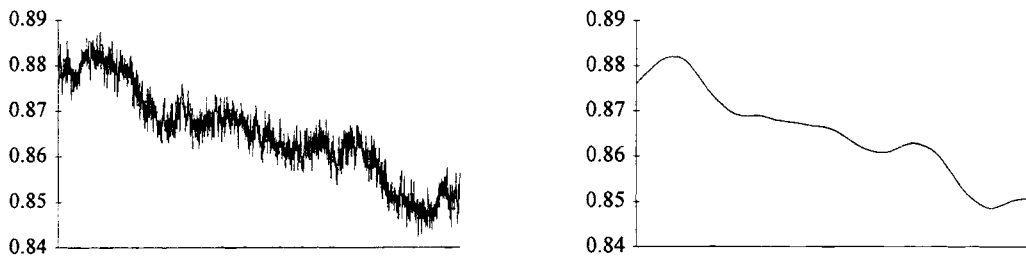


(a)

(b)

Figure 24: Extension with the boundary value, (a) original signal and (b) the extended signal.

Figure 25 shows a signal and the wavelet decomposition when extended using this method.



(a)

(b)

Figure 25: (a) original signal (b) wavelet decomposition using a constant extension method. Note distortion of trend at the boundaries.

In this case also, signal trends are distorted at the boundaries. The decomposed signal shows a smooth trend at the boundaries, contrary to the swings in the original signal.

### **Summary of conventional signal extension methods**

The signal extension methods discussed above are rigid in that they do not take the signal trend patterns into consideration while extending the signal. Stated simply, they are not *adaptive* extension methods and employ the same extension procedure irrespective of the nature of the signal. A better signal extension

technique would be one which adapts itself to suit the specific signal. A signal extension technique that best approximates signal behavior towards the boundaries would provide the best representation.

**The New Extension Technique (NET):** The basic idea behind the development of this approach was to provide a technique that would provide an accurate wavelet decomposition irrespective of the nature of the signal. Unlike the previously described extension methods, the objective of this technique was to provide a reliable extension for all cases.

This method uses a statistical approach to provide a good approximation of the signal outside the boundaries of the signal depending on signal trends at the boundaries. Different statistical approaches were adopted for this purpose and four new extension methods are described in this work.

The concept behind these methods is the same. Signal samples close to the boundary are considered and a mean value is determined. The procedure for determining this “mean value” differs for each of these four methods and each is described in the following sections. The signal is then extended by making it symmetric it with respect to that mean value and then inverting it.

**NET1:** Consider a signal represented by a vector  $a=[a_0 a_1 a_2 a_3 a_4 a_5 a_6 \dots a_n]$ .

A threshold number of samples  $K$  is specified by the user. For illustrative purposes consider  $K=10$ .

Starting from the first value at the left boundary,  $a_0$ , this method calculates the mean

$$f_0=a_0,$$

where  $f_0$  is the mean of the first sample. The sum of the mean squared deviation ( $M_0$ ) of sample  $a_0$  from its mean  $f_0$  is calculated next.

$$M_0=(a_0-f_0)^2=0.$$

Then, the first two samples from the boundary are considered and the mean calculated

$$f_1 = \frac{a_0 + a_1}{2}.$$

The corresponding mean squared deviation of these samples from the mean is calculated

$$M_1 = \frac{(a_0 - f_1)^2 + (a_1 - f_1)^2}{2}.$$

In this way, the procedure is repeated up to  $K$  specified samples, the mean,  $f_i$ , and the mean square deviation from the mean,  $M_i$ , is computed at each step using the following equations :

$$f_i = \frac{\sum_{j=0}^i a_j}{i+1}, \quad i = 0, K-1 \quad (36)$$

$$M_i = \frac{\sum_{j=0}^i (a_j - f_i)^2}{i+1}, \quad i = 0, K-1. \quad (37)$$



A vector of means  $f=[f_1 f_2 f_3 f_4 f_5 f_6 f_7 f_8 f_9 f_{10}.....f_{K-1}]$ , and a vector of mean square deviations from the mean

$M=[M_1 M_2 M_3 M_4 M_5 M_6 M_7 M_8 M_9 M_{10}.....M_{K-1}]$ , is generated. The minimum  $M_i$  is considered and the signal is flipped around the corresponding  $f_i$ .

When  $K=10$ , and  $M_4$  is the minimum mean square deviation, the signal is flipped around  $f_4$ , the mean of the first 4 samples from the boundary. A similar procedure is adopted for the right boundary. In the NET1 method,  $M_i$  is always zero, so the signal is basically flipped around the boundary sample on either side.

The logic behind this approach is that signal trends are approximated well when the signal extension is close to the actual signal trend. The minimum value of mean square deviation is chosen because it is at this value that the sensor signal is more or less representing its basic trend, and deviations are minimum. The signal is flipped and not symmetrically extended because flipping the signal provides a smoother transition across the boundaries and trends are preserved. Figure 26 shows the trend preservation capability of this technique. The left side of the signal follows the downward trend and the right side provides a smooth upward trend.

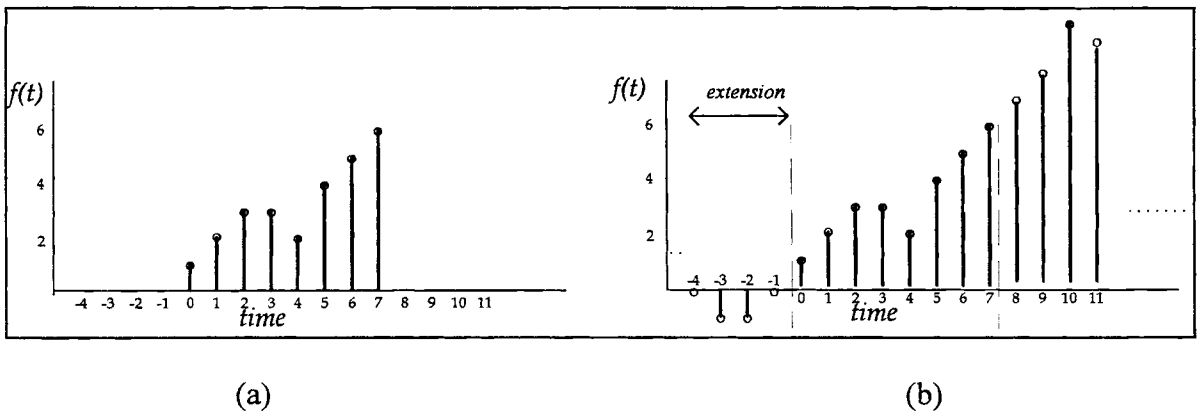


Figure 26: The New Extension Technique, (a) original signal and (b) the extended signal

**NET2:** In this technique, the first 40% of the threshold ( $K$ ) samples are neglected while computing the mean square deviation from the mean. When  $K=10$  as in the previous case, 40% of 10 samples or 4 samples are neglected while computing the minimum  $M_i$ . In equation (36) and equation (37), the index  $i$  would vary from  $0.4K$  to  $K-1$  and not  $0$  to  $K-1$ . The vector for computing the *minimum*  $M_i$  would now be  $M=[M_{0.4K} \ M_{0.4K+1} \ M_{0.4K+2} \dots \dots \dots M_{K-1}]$ . The signal is flipped as in the earlier case around the mean corresponding to the minimum  $M$ .

The first few samples are neglected while computing the mean to flip the signal around because in NET1, the signal is always flipped around the boundary value. This boundary value could contain an unusual amount of noise, and flipping the signal around this point could provide a poor extension.

**NET3:** The vector corresponding to the mean  $f=[f_1 \ f_2 \ f_3 \ f_4 \ f_5 \ f_6 \ f_7 \ f_8 \ f_9 \ f_{10} \dots \dots \dots f_{K-1}]$ , and the vector of the sum of the mean square deviations from the mean

$M=[M_1 \ M_2 \ M_3 \ M_4 \ M_5 \ M_6 \ M_7 \ M_8 \ M_9 \ M_{10} \dots \dots \dots M_{K-1}]$ , are generated as described in the NET1 method. However, in this method, the *maximum value of the mean square deviation (not the minimum value as in NET1)* is considered and the signal flipped with respect to the corresponding mean. For instance, in vector  $M$ , if  $M_6$  corresponds the maximum value, the signal is flipped around the mean  $f_6$ . This method is tailored for signals containing a significant amount of noise. By considering the maximum mean square deviation from the mean, the signal is flipped about a point such that the extended signal fluctuates to its maximum possible extent about the mean trend value. Thus the averaged smoothed version would provide a better representation of the actual trend.

**NET4:** This method is a hybrid of the NET2 and NET3 techniques. The first 40% of the threshold number of samples specified are neglected while computing the

mean around which the signal is flipped. Analogous to the NET3 method, the *maximum* mean square deviation from the mean is used.

Figure 27 illustrates the ways a signal can be extended using the techniques mentioned above. Figure 27(a) shows the original signal. The windows indicate the length to which the signal is extended on either side. Figure 27(b) illustrates the periodic extension method. The signal is extended on the left by using samples in the right window in the original signal; on the right side the signal is extended using samples in the left window. The constant extension method in Figure 27(c) shows extension using the boundary value on either side. Symmetric extension in Figure 27(d) shows the signal flipped with respect to the boundary value. Figures 27(e)-(f) show the NET extension methods, the difference is explicitly represented.

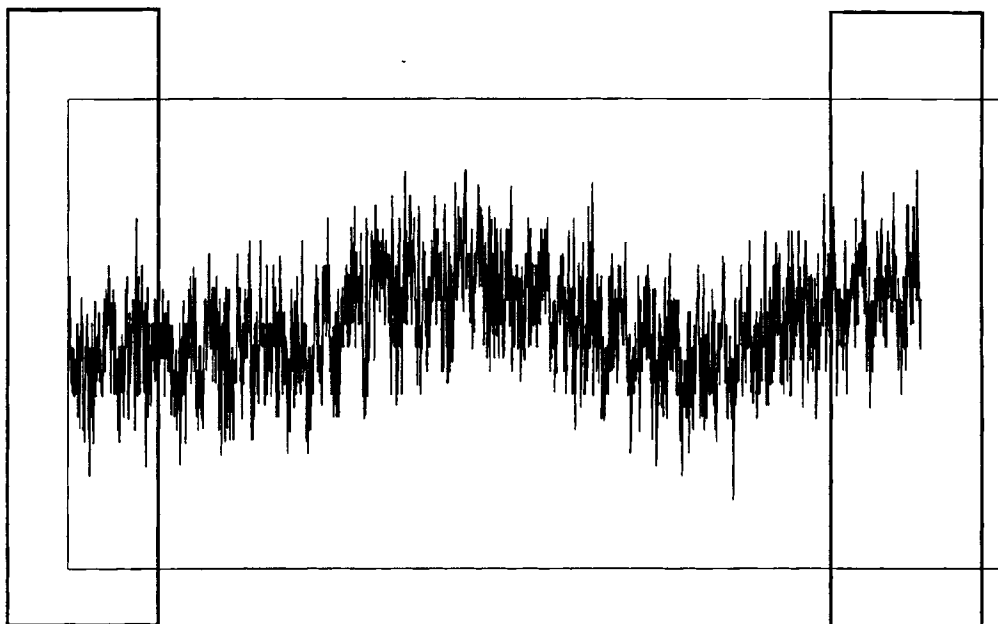


Figure 27(a). The original signal, with the left and right hand side sides

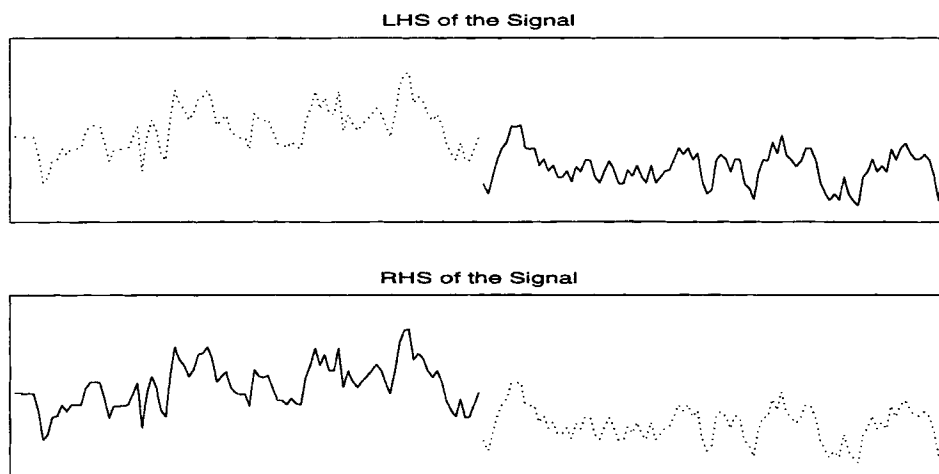


Figure 27(b). Periodic extension on the left and right hand sides

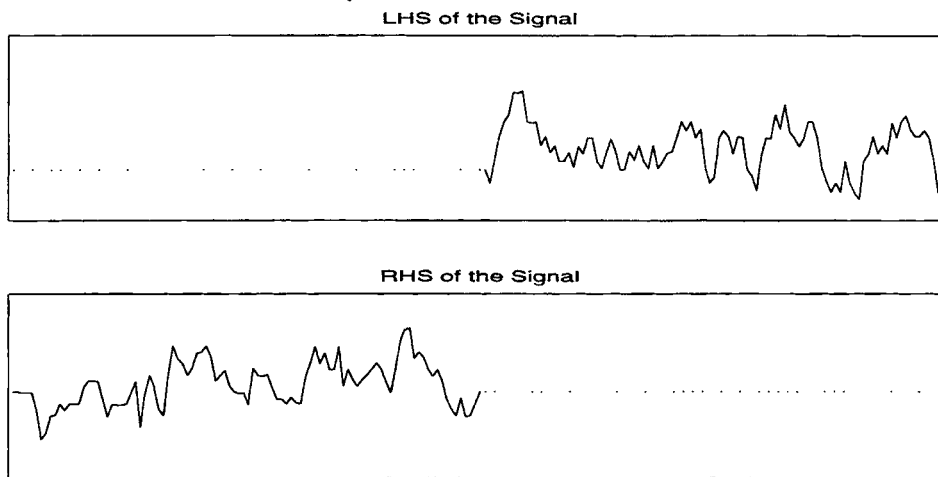


Figure 27(c). Constant extension method on the left and right hand sides

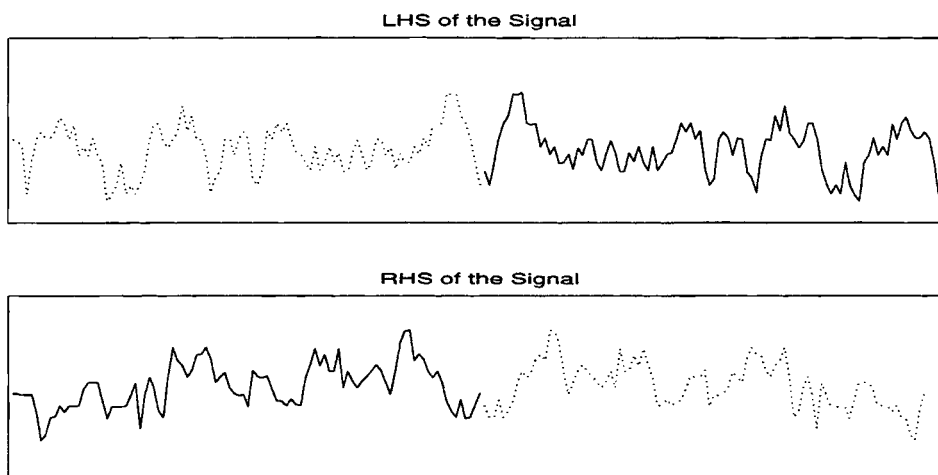


Figure 27(d). Symmetric extension on the left and right hand sides.

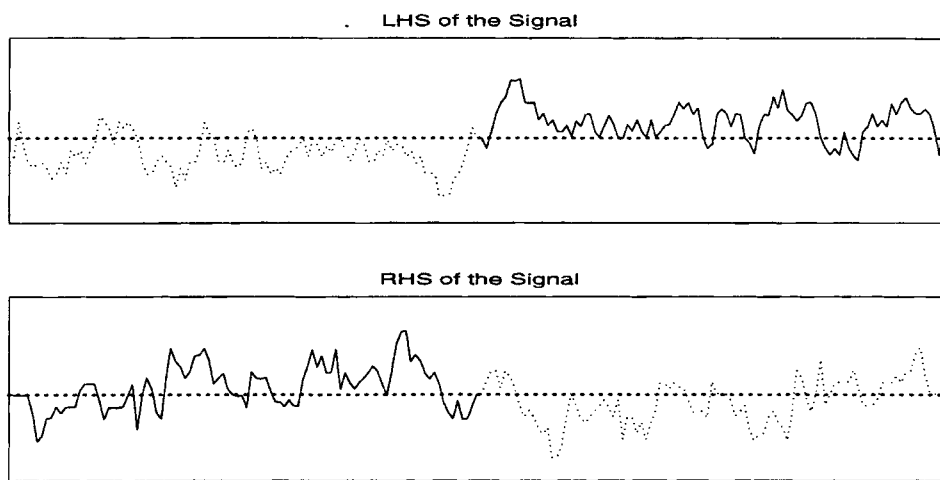


Figure 27(e). The left and right hand sides extended using the NET1 method

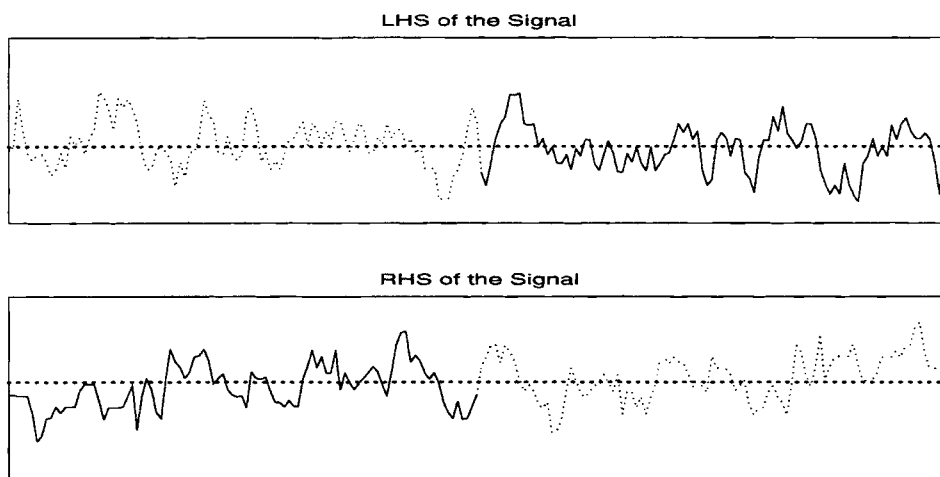


Figure 27(f). The left and right hand sides extended using the NET2 method

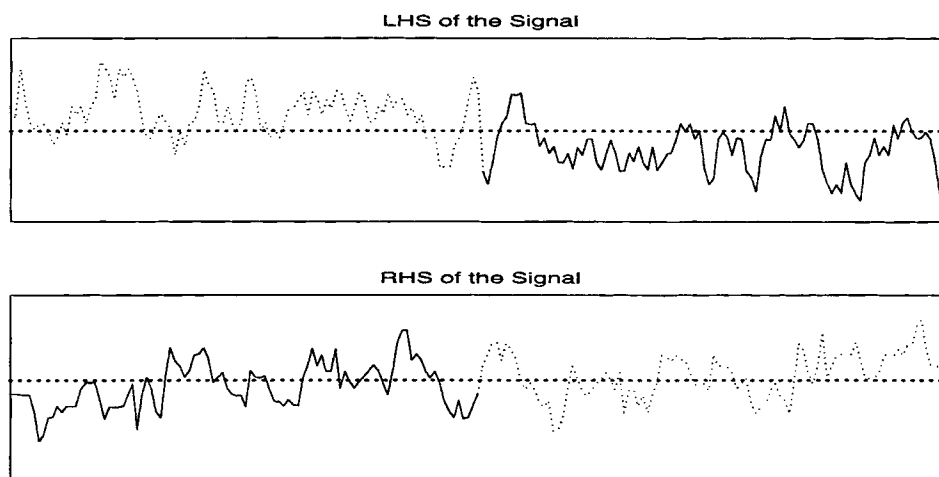


Figure 27(g). The left and right hand sides extended using the NET3 method

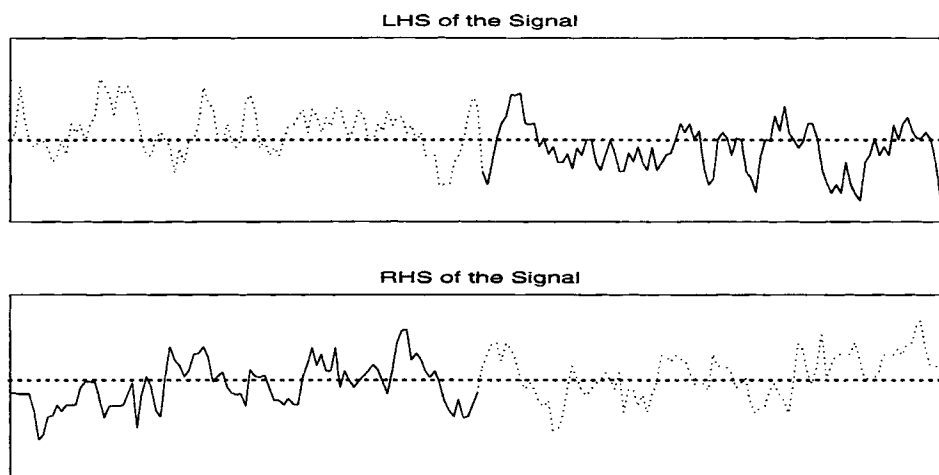


Figure 27(h). The left and right hand sides extended using the NET1 method

Figure 27. The different extension methods

### **Demonstration of NET technique**

To compare these techniques, a set of test signals were sliced into two half-signals, decomposed, reconstructed separately, and reconnected. If this technique works perfectly, the reconstructed signals should match perfectly the original signals. Three process signals were used to test signal extension effectiveness.

**Case I:** A signal with normal swings is considered (Figure 28). This signal is sliced at the crest of one of its swings. This signal is ideal for symmetric extension because the signal is symmetric at the midpoint.

In Figure 28b, the periodic extension method tends to distort the trends of the left slice by raising the pattern above its actual value on the left side of the slice; and a reverse effect occurs on the right side of the slice. Similar pattern distortions are included on the right side of the slice. As a consequence, the boundaries trends to fall either above or below their actual values. When combined, these signals do not provide a smooth transition. The periodic extension method performs poorly, as expected.

The symmetric extension (Figure 28c) performs well in this case due to the nature of the signal. Although this technique provides good representation for the left slice and the left side of the right slice, it smoothes off the right side of the right slice. A flat trend is produced instead of the decrease as in the original case. This distortion is unacceptable for the intended monitoring applications.

The NET1 method is implemented by specifying the threshold number of samples as 1.25% of the total number of samples. Signals in all these test cases each contained 4096 samples, so the domain of search for the mean to flip the signal around was approximately 50 samples. The same threshold is specified for all the NET techniques. Figure 28d shows distortion on left side of the left slice



mainly because there is a high level of noise at the point. Instead of taking the true trend into consideration only signal behavior at the ends is considered.

Consequently, the wavelet decomposition shows a sudden drop on the left side when the true signal trend is flat.

NET2 (Figure 28e) however does a good job of retaining all the trends. In the NET2 method, 40% of the 50 threshold samples or 20 samples are not considered while computing the mean.

NET3 does not provide accurate signal reproduction on the right side of the left slice and the left side of the right slice, resulting in a rough transition at the midpoint in Figure 28f. This technique also shows a slightly rising trend on the left side of the first slice which is contrary to the flat trend in the original signal.

NET4 (Figure 28g) provides an adequate reconstruction, but on the left side of the left hand slice it shows a slightly decreasing trend instead of a flat trend.

For this case, the NET2 was most satisfactory. Only this method retained the essential trend at all the boundaries and provided good reconnection of the two slices.

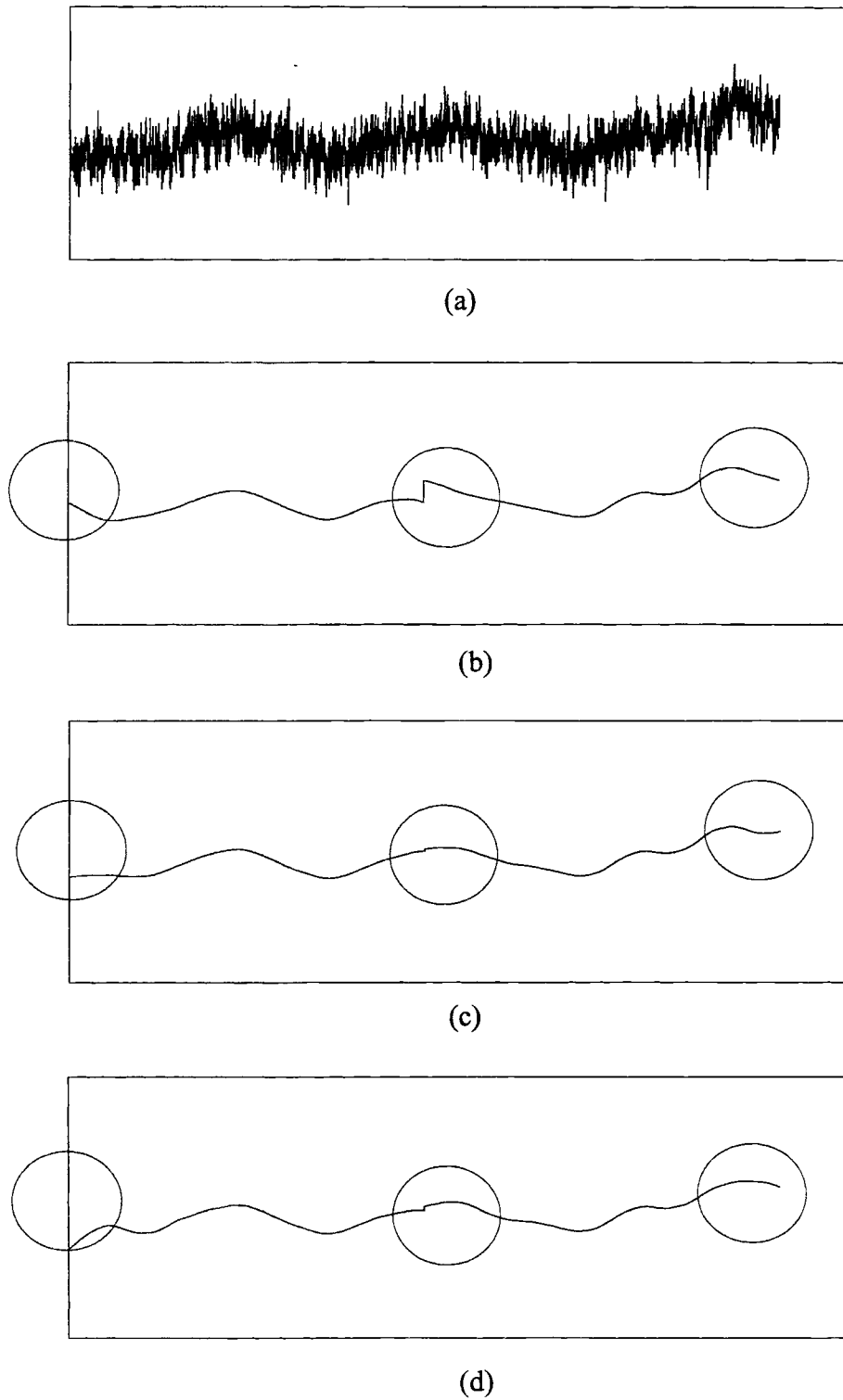
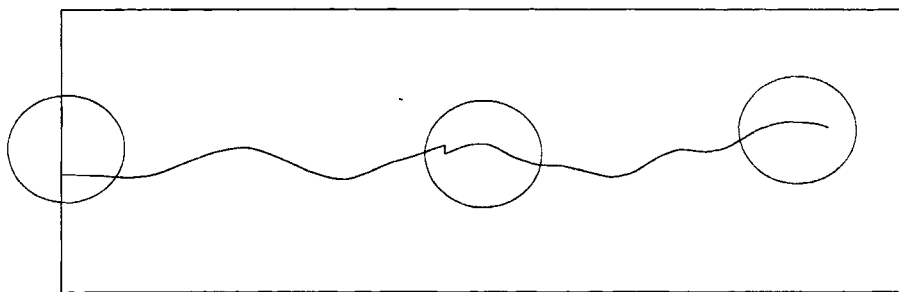
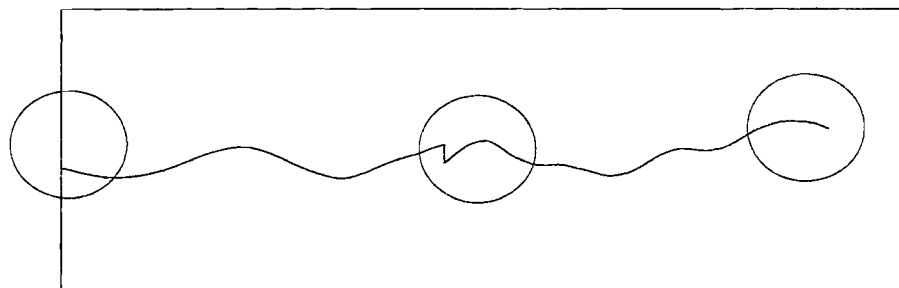


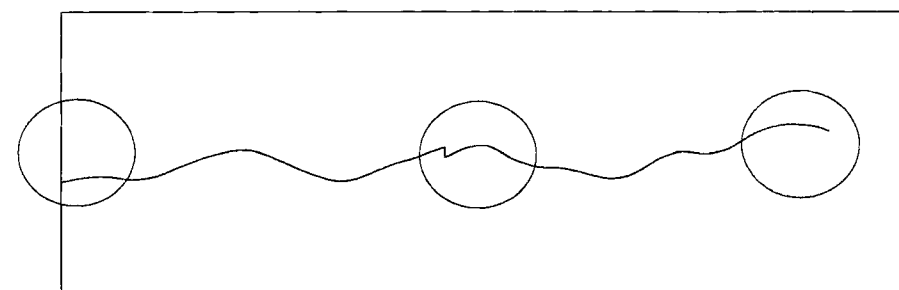
Figure 28: Representation of effect of signal extension on signal combination, (a) original signal (b) using the peridoic extension (c) using the symmetric extension and (d) the New Extension Technique, NET1(threshold is 1.25% of the total signal length)



(e)



(f)



(g)

Figure 28: (contd) (e). using NET2 (f) using NET3 and  
(g) using NET4

**Case II:** A signal with different characteristics is considered in this case (Figure 29). This signal is split into two parts. The first part of the signal has ends that differ significantly. The second part is sliced at points where there are marked changes in the direction of trends. These are analyzed using the afore mentioned techniques and recombined.

Figure 29b shows the periodic extension case. The left boundary of the left slice is significantly above the right boundary, so the trend on the left side of the slice shows a more marked downward change than there actually is. The right side of this slice originally is at a steady value, but is now distorted to indicate a sharp upward change. The direction of the trend on the right side of the right slice is reversed. The periodic extension performs poorly, as expected.

The symmetric extension in Figure 29c performs even worse than the periodic extension method. The left side of the left side does not reflect the gradual rise in the original signal, but shows a sharp rise. The right side of the this slice approaches a constant value when it actually should show a rise. The right slice shows a more gradual drop on the left side of the slice than it actually should. The right side of this slice starts to show a slight rise, where there is none in the original signal. Once again this method is inadequate for our purposes.

The NET1 method in Figure 29d provides excellent trend representation on both sides of the right and the left slices.

The right side of the left slice in NET2 in Figure 29e does not rise as sharply as it should. When the two slices are reconnected, the representation is marginally poorer than in the NET1 case.

NET3 (Figure 29f) also performs poorly on the right side of the left slice. The trend levels off to a greater degree than it actually should, so this method fails for this case.

NET4, shown in Figure 29g, provides a representation comparable to NET2.

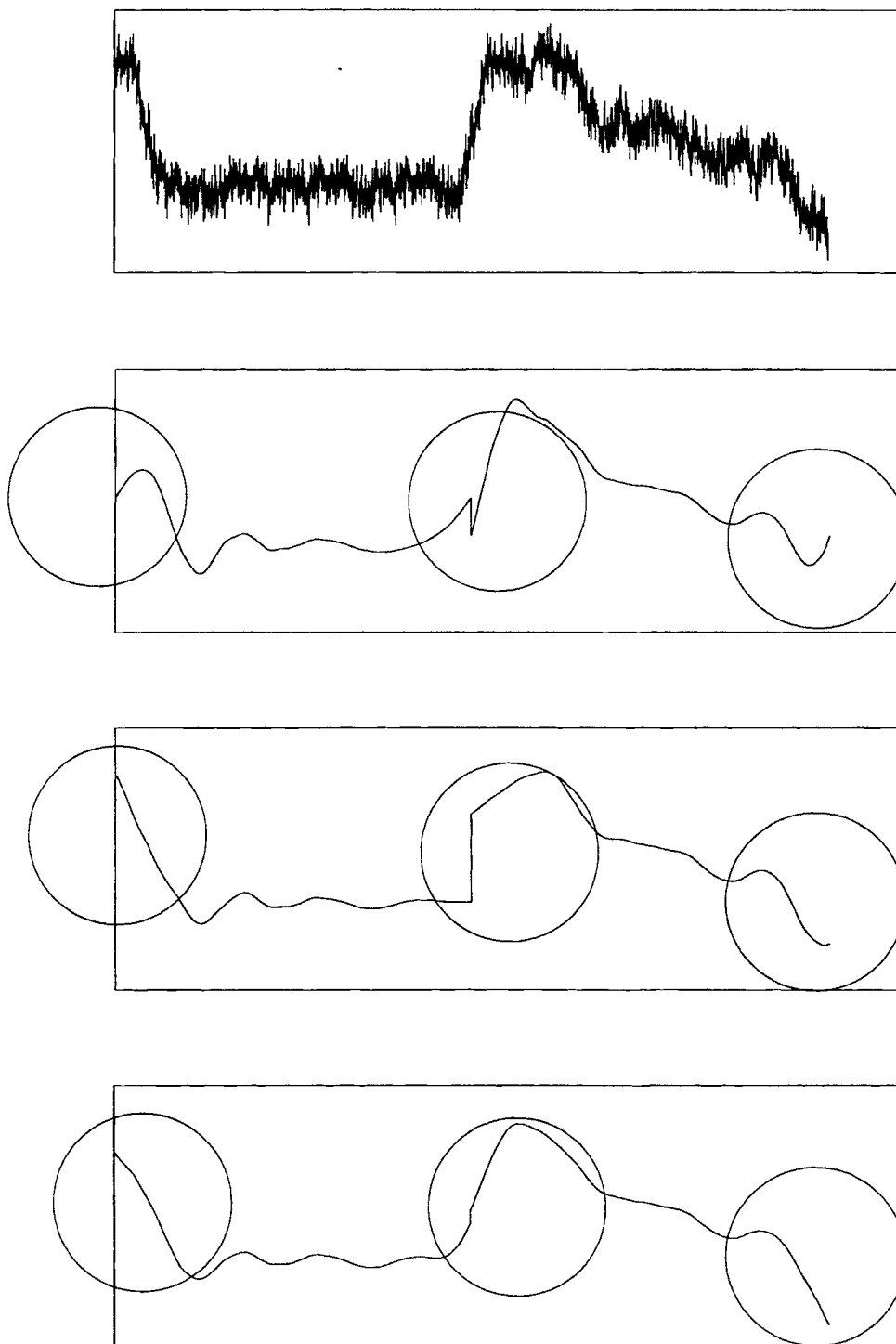


Figure 29: Representation of effect of signal extension on signal combination, (a) original signal (b) using the periodic extension (c) using the symmetric extension and (d) The New Extension Technique

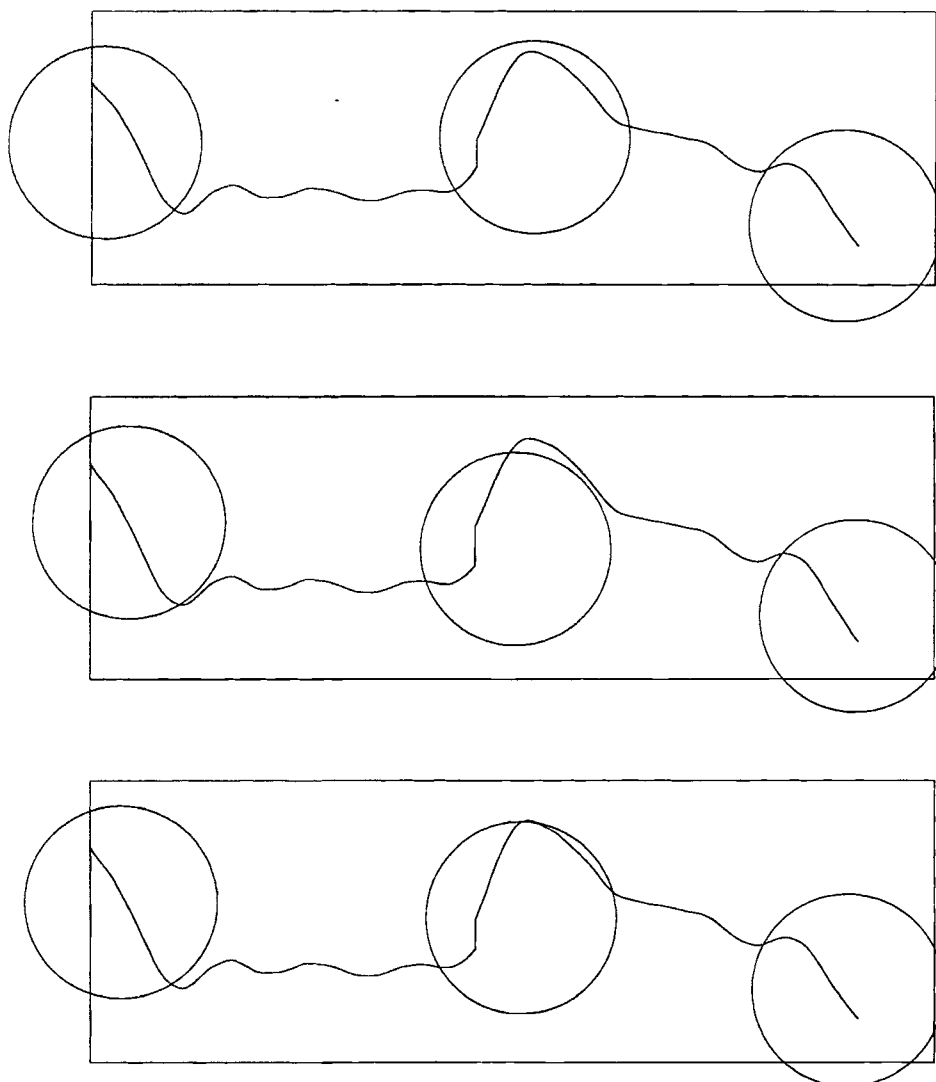


Figure 29 (contd) (e) using NET2 (f) using NET3 and  
(g) using NET4

For Case 2, NET2 and NET1 provide the best representation. The reason NET1 provides a marginally better representation than NET1 is that the trend on the right hand side of the left slice is guided more by samples at the boundary. Since NET2 does not take the immediate vicinity of the boundary into consideration, it fails to replicate the steep trend perfectly but still provides a good representation.

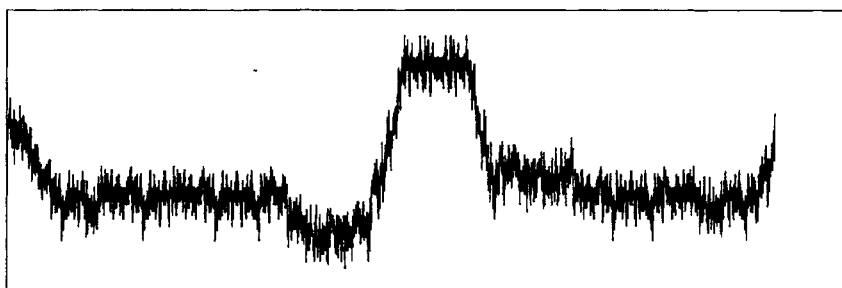
**CASE III:** The right boundary of the process signal in Figure 30 is actually a stray sample, away from the actual process trend. The signal is sliced into half at its midpoint, where the right side of the left slice shows an upward trend.

Since the right and left sides of the left slice are not at identical levels, the left side shows a flat trend when the actual trend is rising. The right hand side of this slice gradually levels off, when actually, it should show a constantly rising trend. The boundaries of the right hand slice are at identical levels, so no significant trend distortion is noticed (Figure 30b) on this side.

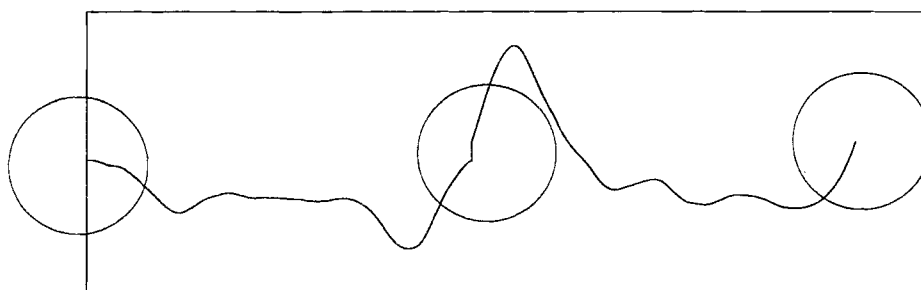
The symmetric extension method (Figure 30c) fails in this case. The left side of the left slice shows a more gradual rise than exists in the original signal. The right side of the slice flattens when it should actually shown an increasing trend. The left side of the right slice shows a marginal drop when actually there is a steep one. Its right side also flattens, when it should show a marginal rise.

The NET1 technique shown in Figure 30d shows perfect trend reconstruction on both sides of the left slice and on the left side of the right slice. However, on the right side of the right slice the influence of the stray boundary sample reflects a sharper trend than there actually is.

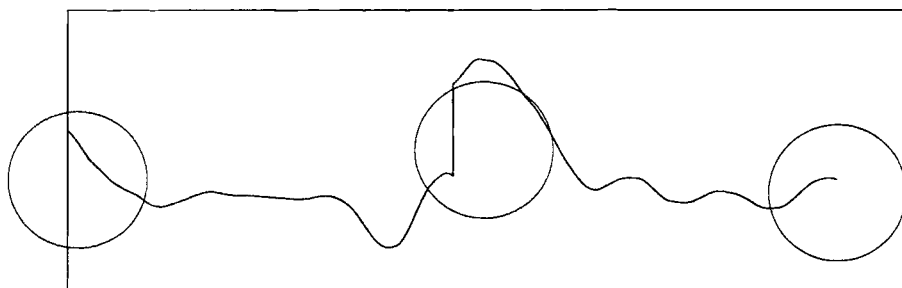
Figure 30e illustrates the NET2 extension method. On the left and right sides of the left slice, trends are represented well. However, at the point of reconnection



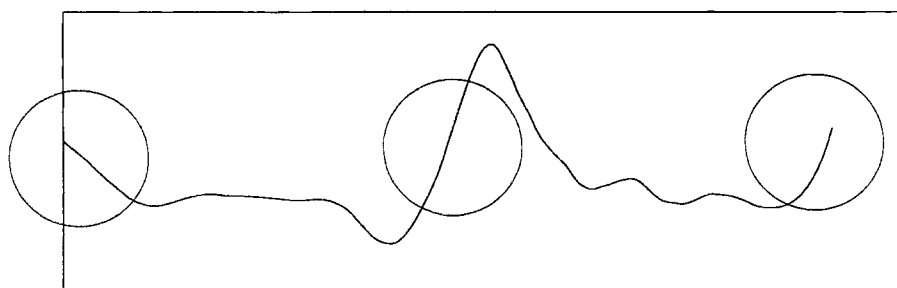
(a)



(b)



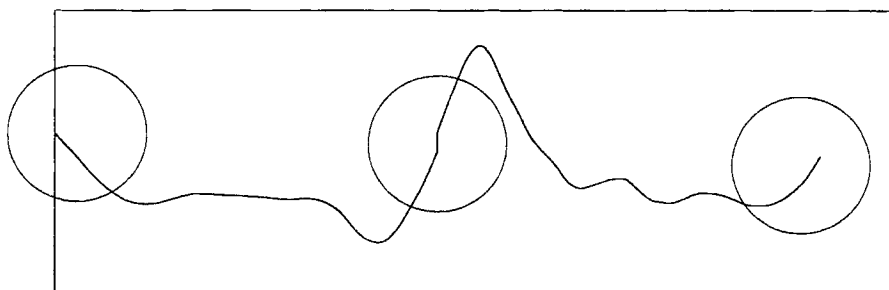
(c)



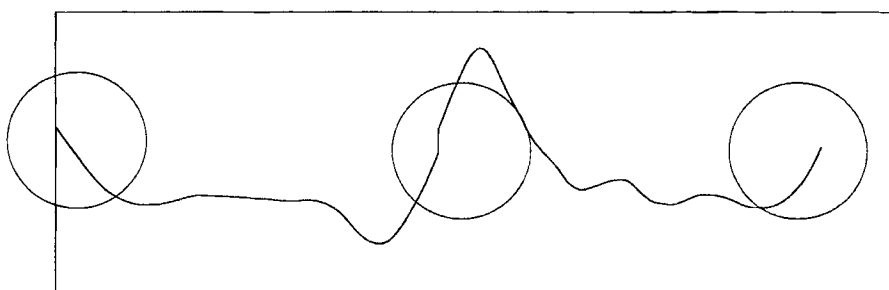
(d)

Figure 30: Representation of effect of signal extension on signal combination, (a) original signal (4096 samples) (b) using the periodic extension (c) using the symmetric extension and (d) The New Extension Technique, NET1

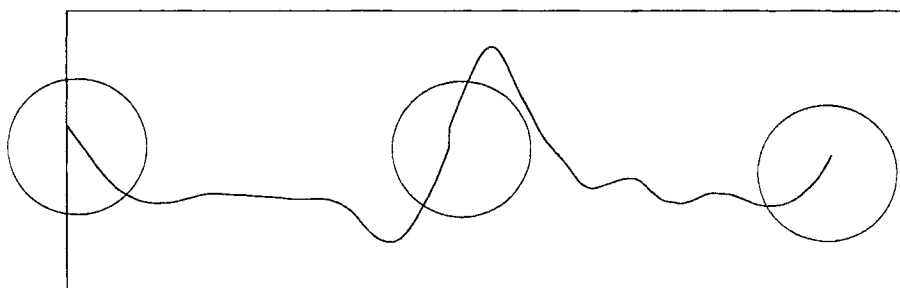




(e)



(f)



(g)

Figure 30: (contd) (e) using NET2 (f) using NET3 and  
(g) using NET4

of these slices, it performs marginally poorer. This method provides a more accurate representation than NET1 on the right side of the right hand slice, because this method ignores samples at the immediate boundaries of the signal.

NET3 (Figure 30f) and NET4 (Figure 30g) provide identical representations because the mean around which the signal is flipped is identical in both cases. They provide good trend representation on both sides of both slices, although at the midpoint they provide a marginally poorer reconnection than NET1 or the NET2 methods.

Considering the fact that the signal extension technique must provide good signal representation and trend retention capability for any signal, it recommended that the NET2 technique be used for compact representation of sensor data used for monitoring and control purposes. NET2 has proved to be a good signal extension method for many cases similar to the test cases presented here.

## **CHAPTER V**

### **CONCLUSIONS**

Though wavelets are new, they have contributed much to signal processing. Most importantly, they provide a much needed alternative to Fourier transforms for certain applications such as pattern based monitoring and control. I have attempted to present the applied aspects of wavelets to the process engineer.

The usefulness of wavelet transforms has been compared and contrasted to Fourier transforms. Effort has been made to provide a technique to extract essential trends from process signals and provide a compact representation. The effectiveness of a signal processing technique depends to a large extent on the nature of the signals involved. One technique that works for specific signal trends might not be effective in dealing with other signal trends. In the pre-processing stage, signal extension has been identified as the critical factor influencing signal representation and retention of trends.

Signal extension is especially important when the application is real-time process monitoring. The signal analysis technique should provide an accurate yet compact representation of the process trend. The ability of a pattern recognition technique to recognize abnormal trends depends on how efficiently the signal is represented and to what extent trend losses are minimized. Trends towards the boundaries are generally indicative of process condition changes and these patterns flag the monitoring technique to detect the change. Thus end effects thus have to be minimized for this technique to be successful.

Some conclusions can also be made about the signal extension techniques when used with wavelet transforms. Periodic extension is simple to implement, but causes serious edge distortions as illustrated in the test cases discussed in the previous chapter. This signal extension technique is completely inappropriate for our needs.

On the other hand, making the signal symmetric at its ends can help minimize the problem of end distortions when the boundaries differ significantly. However, this signal extension technique has a tendency to smooth and flatten trends at the boundaries especially when a process change is just occurring and the direction of the trend is changing. In this case, this method results in a trend that erroneously shows a steady process behavior, masking the trend. This is also unacceptable.

Zero padding and the boundary value extension methods are also inappropriate for our application. Zero padding always results in sharp boundary distortions, while the constant extension method results in the flattening of trends at the boundaries leading to erroneous trend representations.

The NET techniques provide better signal extension than the conventional methods. Their adaptability to signals make them a better proposition for monitoring applications than general techniques like symmetric extension methods.

I have also concluded that NET2 is the best signal extension technique to use in our applications. NET3 and NET4 perform reasonably well in some cases, especially when the signal shows sharp deviations towards the boundaries. The NET1 method performs well in cases that do not exhibit sharp unusual deviations at the ends of the signal. This work recommends the use of NET2 because it provides reasonably accurate reconstruction under any circumstance.

## **Recommendations and Future work**

Future work is required to provide a more theoretical basis to the empirical approach adopted here. The results presented in this work employed parameters based purely on experience and knowledge of the sensor signal behavior. A more generalized technique with a mathematical basis needs to be developed.

Some recommendations are

- More wavelet families need to be studied. This work focused mainly on the Daubechies family of wavelets. Other wavelet families are available and can be used for this purpose. A generalized technique could be developed that determines the most appropriate wavelet family depending on the signal or application.
- At present, the order of wavelet is empirically determined. An automated technique could be developed that takes into account the trend pattern and determines the appropriate order of the wavelet.
- The level of decomposition used for trend pattern extraction is also empirically determined at present. The optimum decomposition level should to be determined and an automated procedure developed.
- To provide better decomposition, the wavelet order could be adaptively modified with the level of decomposition. At the initial stages of decomposition, higher order wavelets can be used. Further down the decomposition tree, lower order wavelets could be applied. This would further minimize distortions due to convolution.
- Currently, the NET technique employs mean square deviation of the signal from the cumulative mean to determine the point with respect to which the signal is extended symmetrically and inverted. A more rigorous statistical technique could provide better signal extension by approximating future samples more accurately. Not only can signal end distortions be avoided this way, but smoother transitions across slices can also be obtained.

- Wavelet packets [Motard and Joseph, 1994] could be investigated to check their performance with the normal decomposition procedures. In the wavelet packet procedure, the detail signal at each level is decomposed further, just like the blurred signal, into two components. After the decomposition is carried to the lowest level, coefficients with the maximum entropy are retained and the remaining deleted. This way data compression is achieved, and signal reconstruction is also accomplished. It needs to be verified though if the reconstruction quality is comparable to the scheme adopted here. The disadvantage is that location of the non-zero coefficients need to be known.
- Instead of using regular decomposition methods, zero crossings of wavelets [Mallat, 1991] can be used to decompose signals. This technique is translation invariant.

## BIBLIOGRAPHY

Akansu, A. N. and R. A. Haddad. *Multiresolution Signal Decomposition : Transforms, Subbands and Wavelets*. Academic Press, Inc., San Diego, CA (1993).

Akansu, A. N., R. A. Haddad and H. Caglar. The binomial QMF -wavelet transform for multiresolution signal decomposition. *IEEE Transactions on Signal Processing* **41**, 13-19 (1993).

Alpert, B. K. Wavelets and Other Bases for Fast Numerical Linear Algebra. *Wavelets: A Tutorial in Theory and Applications*. (C. K. Chui, Eds). Academic Press, Inc, San Diego (1992).

Battle, G. A block spin construction of ondelettes. part I: lemarie functions. *Communications on Mathematical Physics* **110**, 601-615 (1987).

Barnard, H. J., J. H. Weber and J. Biemond. Efficient signal extension for subband/wavelet decomposition of arbitrary length signal. *SPIE Conference on Visual Communications and Image Processing*, , (1993).

Bracewell, R. M. *The Fourier Transform and Its Applications*. McGraw Hill Book Company, (1965).

Brigham, O. E. *The Fast Fourier Transform*. Prentice-Hall, Inc., Eaglewood Cliffs, N.J. (1974).

Chui, C. K. and J.-Z. Wang. A cardinal spline approach to wavelets. *Proceedings of the American Mathematical Society* **113**, 785-793 (1991).

Chui, C. K. and J.-Z. Wang. On compactly supported spline wavelets and a duality principle. *Transactions of the American Mathematical Society* **330**, 903-915 (1992).

Chui, C. K. *An Introduction to Wavelets*. Academic Press, Inc, College Station, Texas (1992a).

Chui, C. K. *Wavelets: A Tutorial in Theory and Applications*. Academic Press, Inc., College Station, Texas (1992b).

Chui, C. K. and J.-Z. Wang. An analysis of cardinal spline wavelets. *Journal of Approximation Theory* **72**, 54-68 (1993).

Cohen, A., I. Daubechies and J. C. Feauveau. Biorthonormal bases of compactly supported wavelets. *Communications on Pure and Applied Mathematics* **45**, 485-560 (1992a).

Cohen, A., I. Daubechies, B. Jawerth and P. Vial. Multiresolution Analysis, Wavelets and Fast Algorithms on an Interval. *C.R Acad. Sci Paris* **316**, 417-421 (1992b).



Cohen, A., I. Daubechies, B. Jawerth and P. Vial. Multiresolution Analysis, Wavelets and Fast Algorithms on an Interval. *C.R Acad. Sci Paris* **316**, 417-421 (1992c).

Combes, J. M., A. Grossmann and P. Tchamitchian. Wavelets:Time-frequency methods and phase space. *Wavelets:Time-frequency methods and phase space Dec 14-18 ,1987*, Marseille,France, (1987).

Daubechies, I. The wavelet transform , time -frequency localization and signal analysis. *IEEE Transactions on Information Theory* **36**, 961-1005 (1990).

Daubechies, I. The wavelet transform: a method for time-frequency localization. *Advances in Spectrum Analysis and Array Processing*. (S. Haykin, Eds). Prentice Hall, Eaglewood Cliffs,New Jersey (1991).

Daubechies, I. *Ten Lectures on Wavelets*. Society for Industrial and Applied Mathematics, Philadelphia (1992).

Daubechies, I. Orthonormal bases of compactly supported wavelets. II variations on a theme. *SIAM Journal of Mathematical Analysis* **24**, 499-519 (1993).

Daubechies, I. and J. C. Lagarias. Two-scale difference equations  
I. existence and global regularity of solutions. *SIAM Journal on Mathematical Analysis* **22**, 1388-1410 (1992a).

Daubechies, I. and J. C. Lagarias. Two-scale difference equations

II. local regularity, infinite products of matrices and fractals. *SIAM Journal on Mathematical Analysis* **23**, 1031-1079 (1992b).

Haykin, S. *Advances in Spectrum Analysis and Array Processing*. Prentice Hall, Eaglewood Cliffs, NJ (1991).

Lemarie, P. G. *Les Ondelettes en 1989*. Springer-Verlag, Berlin (1990).

Lemarie, P. P.-G. Ondelettes a localisation exponentielle. *Journal de mathematiques pures et appliquees* **67**, 227-236 (1988).

Mallat, S. G. Multifrequency channel decomposition of images and wavelet models. *IEEE Transactions on Acoustics ,Speech and Signal Processing* **37**, 2091-2110 (1989a).

Mallat, S. G. Multiresolution approximations and wavelet orthonormal bases of  $L_2(\mathbb{R})$ . *Transactions of the American Mathematical Society* **315**, 69-87 (1989b).

Mallat, S. G. A theory for multiresolution signal decomposition: the wavelet representation. *IEEE Trans. Pattern Anal. Mach. Intellig.* **2**, 674-693 (1989c).

Mallat, S. Zero-crossing of a wavelet transform. *IEEE Transactions on Information Theory* **37**, 1019-1033 (1991).

Meyer, Y. Principe d'incertitude, bases hilbertinnes et algebres d'operateurs. *Seminaire Bourbaki, 1985-1986, no. 662*. Eds). Societe Mathematique de France, (1985).

Motard, R. L. and B. Joseph. *Wavelet Applications in Chemical Engineering*. Kluwer Academic Publishers, Norwell, MA (1994).

Oslen, P. A. and K. Seip. A note on irregular discrete wavelet transform. *IEEE Transactions on Information Theory* **38**, 861-863 (1992).

Papoulis, A. *Signal Analysis*. McGraw Hill, (1977).

Rice, J. R. *The Approximation of Functions*. Addison-Wesley Publishing Company, Warren, Michigan (1964).

Rioul, O. and M. Vetterli. Wavelets and signal processing. *IEEE SP Magazine* 14-35 (1991).

Ruskai, M. B. *Wavelets and their applications*. Jones and Barlett publishers, Boston (1992).

Smith, M. J. T. and S. L. Eddins. Analysis/synthesis techniques for subband image coding. *IEEE Transactions on Acoustics, Speech and Signal Processing* **38**, 1446-1456 (1990).

Strang, G. Wavelets and dilation equations : A brief introduction. *Society for Industrial and Applied Mathematics* **31**, 614-627 (1989).

Strang, G. Wavelet transforms versus fourier transforms. *Bulletin of the American Mathematical Society* **28**, 288-305 (1993).

Strichartz, R. S. How to make wavelets. *The American Mathematical Monthly* **100**, 539-556 (1993).

Walter, G. G. A sampling theorem for wavelet subspaces. *IEEE Transactions on Information Theory* **38**, 881-884 (1992).

Weaver, J. H. *Applications of Discrete and Continuous Fourier Analysis*. John Wiley & Sons, (1983).

## **APPENDIXES**

## **APPENDIX A**

Computing the scaling function and wavelet coefficients  
for the Daubechies family of wavelets

The Fourier transform of a function  $f(t)$  is defined as

$$\hat{f}(\xi) = \frac{1}{\sqrt{2\pi}} \int e^{-i\xi t} f(t) dt \quad (38)$$

The Fourier transform of (6) gives,

$$\frac{1}{\sqrt{2\pi}} \int e^{-i\xi x} \varphi(t) dt = \frac{1}{\sqrt{2\pi}} \sum_k c_k \int e^{-i\xi x} \varphi(2t - k) dt,$$

$$\hat{\varphi}(\xi) = \frac{1}{2} \sum_k c_k e^{-ik\xi/2} \hat{\varphi}\left(\frac{\xi}{2}\right) \quad (39)$$

$$\text{Define } m_0(\xi) = \frac{1}{2} \sum_k c_k e^{-ik\xi}, \quad (40)$$

$$\text{then } \hat{\varphi}(\xi) = m_0\left(\frac{\xi}{2}\right) \hat{\varphi}\left(\frac{\xi}{2}\right) \quad (41)$$

equation (40) indicates that  $m_0(\xi)$  is a function, a periodic function with a period  $2\pi$ .

It also gives another set of boundary conditions, for  $\xi = 0$  and  $\xi = \pi$ . For  $\xi = 0$ , equation (40) gives

$$\begin{aligned} m_0(0) &= \frac{1}{2} \sum_k c_k e^{-i \cdot 0 \cdot k} = \frac{1}{2} \sum_k c_k \cdot \{\cos(0) - i \sin(0)\} \\ &= \frac{1}{2} \sum_k c_k \cdot 1 = 1 \end{aligned}$$

because  $\sum_k c_k = 2$ . Similarly, for  $\xi = \pi$ , (40) gives

$$\begin{aligned} m_0(\pi) &= \frac{1}{2} \sum_k c_k e^{-i \cdot \pi \cdot k} = \frac{1}{2} \sum_k c_k \{\cos(\pi k) - i \sin(\pi k)\} \\ &= \frac{1}{2} \sum_k c_k \cdot (-1)^k = \frac{1}{2} \sum_k d_k = 0 \end{aligned}$$

So,

$$m_0(0) = 1, m_0(\pi) = 0 \quad (42)$$

The orthonormality of  $\phi$  also yields the following relationship, explanation for this can be found in p132 of [Daubechies, 1992].

$$\sum_l |\hat{\phi}(\xi + 2\pi l)|^2 = (2\pi)^{-1} \quad (43)$$

substitute (41) into (43), the result is

$$\sum_l |\hat{\phi}(\frac{\xi}{2} + \pi l)|^2 |m_0(\frac{\xi}{2} + \pi l)|^2 = (2\pi)^{-1}. \quad (44)$$

Split (44) into odd and even terms. The following equation results from the LHS of (44)

$$\sum_l |\phi(\frac{\xi}{2} + 2\pi l)|^2 |m_0(\frac{\xi}{2} + 2\pi l)|^2 + \sum_l |\phi(\frac{\xi}{2} + (2l+1)\pi)|^2 |m_0(\frac{\xi}{2} + (2l+1)\pi)|^2. \quad (45)$$

The fact that  $m_0$  is periodic is used now to simplify the expression given above. The simplification is of the form

$$|m_0(\frac{\xi}{2})|^2 \sum_l |\hat{\phi}(\frac{\xi}{2} + 2\pi l)|^2 + |m_0(\frac{\xi}{2} + \pi)|^2 \sum_l |\hat{\phi}(\frac{\xi}{2} + 2\pi l + \pi)|^2 \quad (46)$$

$$= (2\pi)^{-1} \left[ |m_0(\frac{\xi}{2})|^2 + |m_0(\frac{\xi}{2} + \pi)|^2 \right] \quad (47)$$



Therefore the result is

$$\left| m_0\left(\frac{\xi}{2}\right) \right|^2 + \left| m_0\left(\frac{\xi}{2} + \pi\right) \right|^2 = 1 \quad (48)$$

Define  $z = e^{-i\xi}$ , also define

$$m_0(\xi) = \frac{1}{2} \sum_k c_k z^k = P(z) \quad (49)$$

It is possible to define (48) in terms of  $P(z)$  as

$$|P(z)|^2 + |P(-z)|^2 = \quad (50)$$

To form an orthonormal basis of wavelets,  $m_0$  is defined as in equation (51). The mathematically sophisticated reader is referred to corollary 5.5.4 on pp. 155-156 in [Daubechies, 1992].

$$m_0(\xi) = P(z) = \left( \frac{1+z}{2} \right)^N E(z) \quad (51)$$

where  $E(1) = 1$ , and  $E(z)$  is the Polynomial with *real coefficients*. The reason why real coefficients are chosen is because real numbers are easier to deal with. Therefore  $|E(e^{-i\xi})|^2$  is a *cosine* polynomial. Taking

$$|E(e^{-i\xi})|^2 = \tilde{R}(\cos \xi) \quad (52)$$

where  $R$  is a polynomial, again with *real* coefficients. Take  $t = \cos \xi = \sin^2\left(\frac{\xi}{2}\right)$  ;

$$R(t) = \tilde{R}(\cos \xi) = \tilde{R}(1-2t) \quad (53)$$

since  $|P(z)|^2 + |P(-z)|^2 =$  from (50), on substituting the value of  $P(z)$  from (51), the result is

$$\left| \left( \frac{1+z}{2} \right)^N \right|^2 |E(z)|^2 + \left| \left( \frac{1-z}{2} \right)^N \right|^2 |E(-z)|^2 = 1 \quad (54)$$

put  $t = \cos \xi$ ,

$$(1-t)^N R(t) + t^N R(1-t) = 1 \quad (55)$$

The general solution to an equation like (55) is

$$R(t) = \sum_{k=0}^{N-1} \binom{N-1+k}{k} t^k + t^N \tau(t) \quad (56)$$

where  $\tau(1-t) = -\tau(t)$  and  $\tau_0(t) = \tau\left(\frac{1-2t}{2}\right)$ .

For further mathematical details, the reader is directed to pp. 175-176 in [Chui, 1992a]. So,

$$\left| E(e^{-i\xi}) \right|^2 = \sum_{k=0}^{N-1} \binom{N-1+k}{k} \left( \sin \frac{\xi}{2} \right)^{2k} + \left( \sin \frac{\xi}{2} \right)^{2N} \tau_0\left(\frac{\cos \xi}{2}\right) \quad (57)$$

$\tau_0$  is an odd polynomial. Choosing  $\tau_0$  equal to zero gives scaling functions with minimum number of coefficients for any given  $N$ . Due to this assumption, (57) narrows down to

$$|E(e^{-i\xi})|^2 = \sum_{k=0}^{N-1} \binom{N-1+k}{k} \left(\sin \frac{\xi}{2}\right)^{2k} \quad (58)$$

the problem now is to solve (58) for  $E(e^{-i\xi})$ . To do this the Riesz Lemma is used. A proof of this lemma can be found in pp. 232-233 in [Chui, 1992a]. Once  $E(e^{-i\xi})$  is calculated, then  $P(z)$  is calculated by equation (51) which then gives the values of the coefficients of the scaling function.

Then the wavelet filter coefficients are calculated from the QMF relationship. This procedure is elucidated for the construction of a wavelet of the Daubechies family.

$$|E(e^{-i\xi})|^2 = \sum_{k=0}^{2-1} \binom{2-1+k}{k} \left(\sin \frac{\xi}{2}\right)^{2k}$$

$$= +2\sin^2 \frac{\xi}{2}.$$

Now  $\sin^2 \frac{\xi}{2}$  is  $-\cos \xi = 1 - \left(\frac{z+z^{-1}}{2}\right)$ . So,

$$|E(e^{-i\xi})|^2 = \frac{1}{2}(-z^{-1} + 4 - z) = \frac{z^{-1}}{2}(-1 + 4z - z^2)$$

The roots of this equation are  $z = 2 \pm \sqrt{3}$ , the root within the unit circle is chosen. Then  $|E(e^{-i\xi})|$  is calculated as shown

$$|E(e^{-i\xi})| = \frac{1}{\sqrt{2}\sqrt{2+\sqrt{3}}} (z - (2+\sqrt{3})) = \frac{1}{2} ((\sqrt{3}-1)z - (\sqrt{3}+1))$$

Then from equation (51),  $P(z)$  is calculated as follows

$$\begin{aligned}
 P(z) &= \left(\frac{1+z}{2}\right)^2 \frac{1}{2} \left( (\sqrt{3}-1)z - (\sqrt{3}+1) \right) \\
 &= \frac{1}{2} \left( \frac{1+\sqrt{3}}{4} + \frac{3+\sqrt{3}}{4}z + \frac{3-\sqrt{3}}{4}z^2 + \frac{1-\sqrt{3}}{4}z^3 \right)
 \end{aligned}$$

comparing with equation (49) the coefficients are obtained.

$$c_0 = \frac{1+\sqrt{3}}{4}; c_1 = \frac{3+\sqrt{3}}{4}; c_2 = \frac{3-\sqrt{3}}{4}; c_3 = \frac{1-\sqrt{3}}{4}.$$

The wavelet coefficients are obtained by the QMF relationship, to give

$$d_0 = \frac{1-\sqrt{3}}{4}; d_1 = -\frac{3-\sqrt{3}}{4}; d_2 = \frac{3+\sqrt{3}}{4}; d_3 = -\frac{1+\sqrt{3}}{4}$$

Similarly the coefficients can be calculated for higher orders of wavelets.

## **APPENDIX B**

### Computing signal decomposition coefficients

Consider an infinitely long signal. The signal is approximated as given in equation (1).

$$f_0(t) = \sum_{k=-\infty}^{\infty} a_k^0 \phi_k^0(t) \quad (59)$$

$$= \sum_{k=-\infty}^{\infty} a_k^1 \phi_k^1(t) + \sum_{k=-\infty}^{\infty} b_k^1 \psi_k^1(t) \quad (60)$$

Here  $a_k^0$  is the vector that approximates the signal at the original resolution,  $a_k^1$  and  $b_k^1$  are the blurred and detail coefficients at the first level.

Multiply both sides by  $\phi_k^1(t)$  and integrate ,

$$a_k^1 = \sum_{k=-\infty}^{\infty} a_k^0 \int_{-\infty}^{\infty} \phi_k^0(t) \phi_k^1(t) dt \quad (61)$$

Similarly on multiplying by  $\psi_k^1(t)$  and integrating

$$b_k^1 = \sum_{k=-\infty}^{\infty} a_k^0 \int_{-\infty}^{\infty} \phi_k^0(t) \psi_k^1(t) dt \quad (62)$$

Since  $c_k = \int_{-\infty}^{\infty} \phi_k^0(t) \phi_k^1(t) dt$  and  $d_k = \int_{-\infty}^{\infty} \phi_k^0(t) \psi_k^1(t) dt$ , the resultant equation

$$a_k^1 = \sum_{k=-\infty}^{\infty} a_k^0 c_k; \quad b_k^1 = \sum_{k=-\infty}^{\infty} a_k^0 d_k. \quad (63)$$

For finite length sequences, the limits on the summation are also finite.

## VITA

**Vinod Kumar Raghavan**

Candidate for the Degree of

Master of Science

**Thesis: WAVELET REPRESENTATION OF SENSOR SIGNALS FOR  
MONITORING AND CONTROL**

Major Field: Chemical Engineering

Biographical:

Personal Data: Born in Visakhapatnam, Andhra Pradesh, India, February 1, 1971, the son of K.G.Srinivasa and Kamala Raghavan.

Education: Graduated from Keshav Memorial Junior College, Hyderabad, AP, India, in May 1988; received Bachelor of Science Degree in Chemical Engineering from Osmania University, Hyderabad, India, in May 1992; completed requirements for the Master of Science degree at Oklahoma State University in May 1995.

Professional Experience: Teaching Assistant, School of Chemical Engineering, Oklahoma State University, August 1992, to December 1992; Research Assistant, School of Chemical Engineering, Oklahoma State University, January 1993, to June 1994.